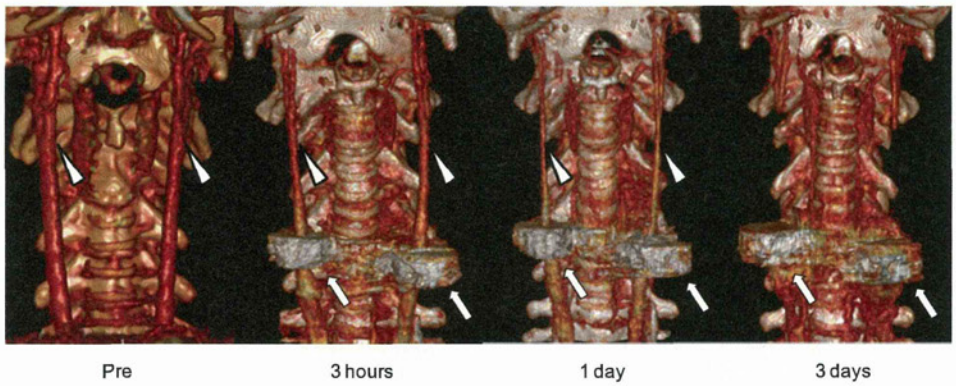

Fig. 3. Three-dimensional volume-rendered images of computed tomography (CT)-angiography showing the blood flow of the bilateral common carotid arteries pre- and postimplantation of ameroid constrictors at indicated time intervals. Arrowheads indicate common carotid arteries and arrows ameroid constrictors.

were assessed by quantitative real-time RT-PCR (Supplemental Method VIII).

2.10. Enzyme-linked immunosorbent assay (ELISA) for TNF-α

The protein concentration of TNF-α in brain homogenates were also measured using a specific ELISA kit according to the manufacturer's recommendation (R&D Systems, Minneapolis, MN, USA) (Supplemental Method IX).

2.11. Western blotting analysis for myelin basic protein

The optic nerves and chiasma were analyzed for demyelinating changes. A rabbit anti-MBP antibody and a mouse anti β-actin antibody (which served as an internal control), were used (Supplemental Method X).

2.12. Y-maze test for spatial working memory assessment

Spatial working memory was assessed by the Y-maze test (Supplemental Method XI).

2.13. Statistical analysis

All values are expressed as mean ± standard error of the mean (SEM). One-way analysis of variance was used to evaluate significant differences among groups (except where otherwise stated) followed by a post hoc Tukey test or Tukey-Kramer test. Differences with $p < 0.05$ were considered significant in all statistical analyses.

3. Results

3.1. Mortality rates and body weight changes of rats

The mortality rate in the 2VGO group was 2.0% (1/49). This was much lower than that of the 2VO group, which was 13.8% (8/58), in accordance with previous reports (Fujishima et al., 1976). In the sham group, all 48 rats survived until euthanized. Body weight decreased in both the 2VGO and 2VO groups, which was significantly less severe in the 2VGO group at 1 day postoperation (2VGO group, −14.1 ± 2.0% vs. 2VO group, −27.4 ± 1.7%; $p < 0.01$). Both groups of rats started to regain body weight at 3 days.

3.2. Gradual narrowing of the common carotid arteries

Bilateral placement of the ameroid constrictors on the CCAs produced the expected narrowing of the inner lumen: 0.28 mm at 1 day postoperation, 0.24 mm at 3 days, and 0.19 mm at 5 days (Fig. 1B and C). CTA indicated that blood flow of CCAs distal to the implanted ameroid constrictors did not decrease at 1 hour but started to decrease at 3 hours, leading to complete occlusion of the CCAs at 3 days (Fig. 3).

3.3. Temporal profiles of CBF recorded by LSF

In the 2VO group, CBF dropped sharply to 55.2 ± 0.8% of the baseline level at 3 hours postoperation but started to recover at 3 days and reached to 85.6 ± 3.7% at 28 days. In contrast, in the 2VGO group, the acute phase observed in the 2VO group was absent; CBF did not decrease at 1 hour (102.5 ± 2.9%) but started to decrease at 3 hours (79.6 ± 3.3%), and reached a minimum at 3 days (69.3 ± 1.7%), before gradually recovering at 28 days (84.5 ± 3.3%). In the sham group, no apparent change of CBF was detected. Two-way repeated measures analysis of variance showed a significant interaction between group and time ($F(14,63) = 16.976$; $p < 0.001$) and significant differences between the 2VGO and 2VO groups at 1, 3, and 6 hours, and 1 day (Fig. 4).

The blood pressure and pulse rate of the surviving rats did not differ significantly among the 3 groups at any postoperative intervals until 28 days.

3.4. ^{18}F-FDG PET analysis

The first 5-minute uptake of ^{18}F-FDG, which was used as an indicator of CBF, showed a similar temporal profile of the CBF recorded by LSF: the uptake dropped more sub-

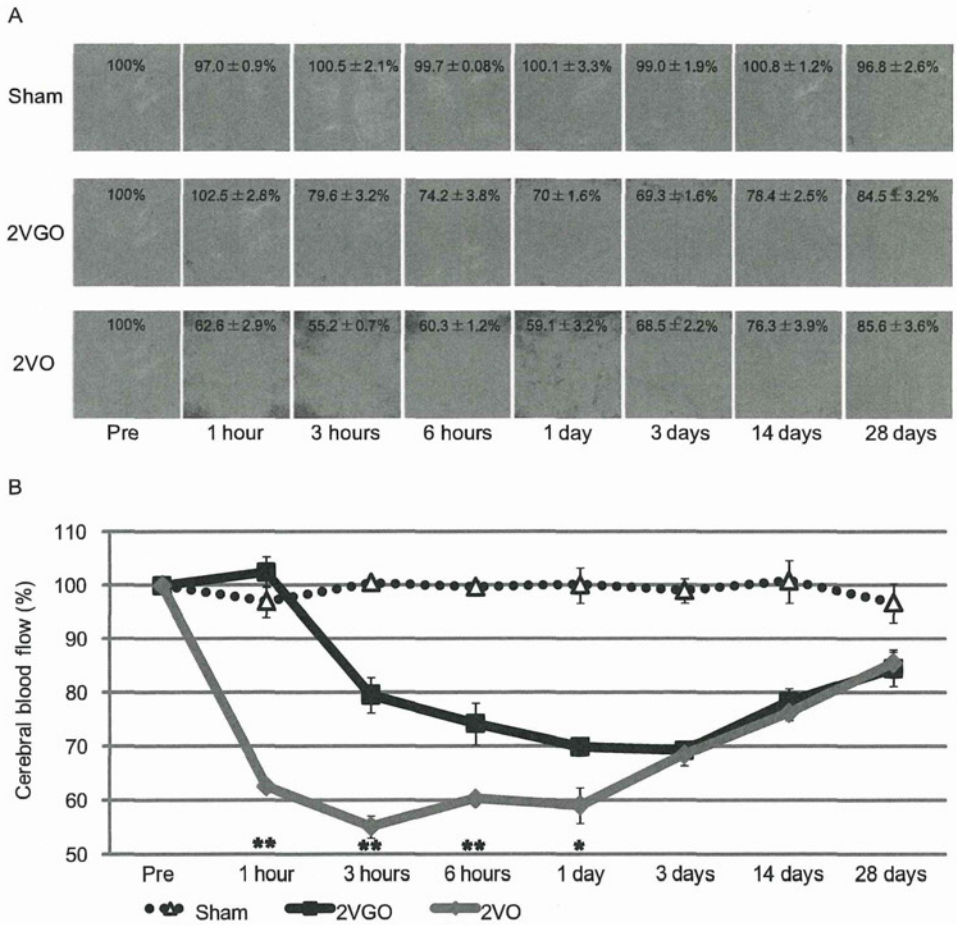

Fig. 4. (A) Representative cerebral blood flow (CBF) images of laser speckle flowmetry in each group at indicated time intervals. The value in each image indicates relative CBF that is expressed as a percentage ± standard error of the mean (SEM) of the baseline level (100%). Four to 6 animals in each group were used at each point. (B) The temporal profile of CBF in each group. * $p < 0.05$, ** $p < 0.01$, 2-vessel gradual occlusion (2VGO) versus 2-vessel occlusion (2VO).

stantially in the 2VO than 2VGO groups at 3 hours postoperation but recovered at 28 days in both groups (Fig. 5A).

The late ^{18}F-FDG uptake, used as an indicator of cerebral glucose metabolism, did not significantly decrease at 28 days in the 2VGO group, whereas in the 2VO group at 28 days, late ^{18}F-FDG uptake significantly decreased in the cerebral cortex compared with that in the 2VGO group and in the hippocampus compared with preoperation (Fig. 5B).

3.5. Y-maze test for spatial working memory assessment

In the 2VGO and 2VO groups, the percentage of alternation behaviors (used as a reflection of spatial working memory) was significantly decreased (Fig. 6A), whereas the number of arm entries was significantly increased, compared with the sham group at 28 days (Fig. 6B).

3.6. Histological analysis of gray matter damage

Brain infarcted areas were not found in any rats of the 2VGO and sham groups but in 50% of rats in the 2VO group at 3, 14, and 28 days (Supplemental Fig. 1A). The infarctions were distributed mainly in the caudoputamen. Cortical gliosis was not found in the sham group and was present in only 8.3% of rats in the 2VGO group at 3, 14, and 28 days (Supplemental Fig. 1B); however, cortical gliosis was present in 75% of rats in the 2VO group over the same periods. There was a trend toward increased density of pyknotic neurons in the hippocampal CA1 region at 28 days in the 2VO group compared with the 2VGO and sham groups (Supplemental Fig. 1C); however, there were no significant differences in density among the 3 groups.

3.7. Histological analysis of white matter damage

Quantitative analysis of the grading score of Klüver-Barrera staining of the corpus callosum indicated that the white matter damage was significantly more severe in both the 2VGO and 2VO groups compared with the sham group at 28 days postoperation; however, the extent of damage was significantly smaller in the 2VGO compared with 2VO groups (Fig. 7A). Similar findings in the degree of myelin damage (assessed by dMBP staining) (Fig. 7B) and the

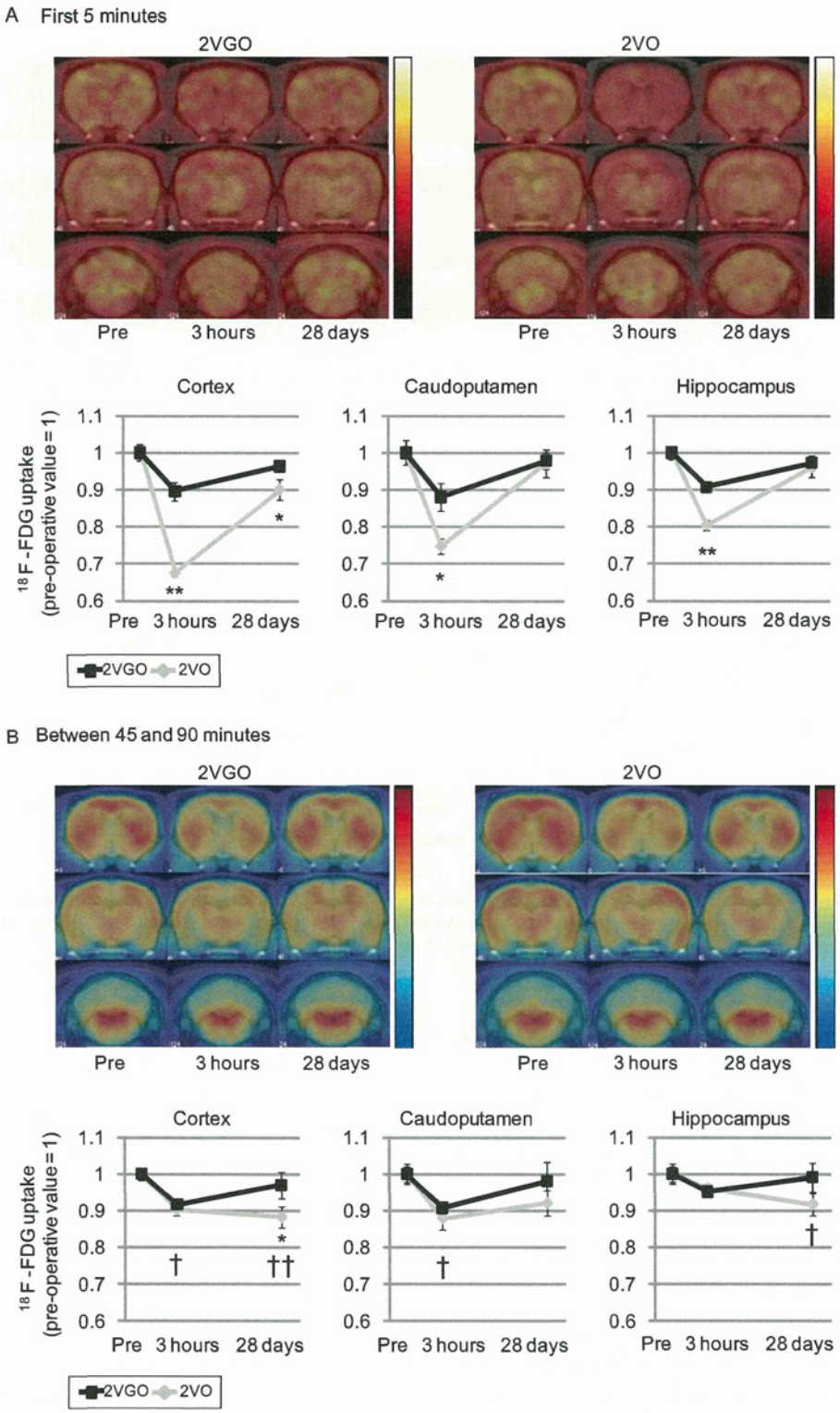

Fig. 5. (A) Representative ^{18}F-fluorodeoxyglucose (FDG) positron emission tomography (PET) coronal images superimposed on magnetic resonance (MR) images for the first 5 minutes of the 2-vessel gradual occlusion (2VGO) (upper left panels) and 2-vessel occlusion (2VO) (upper right panels) groups. Temporal profiles of the mean normalized ^{18}F-FDG count during the first 5 minutes in the cerebral cortex (lower left), caudoputamen (lower middle), and hippocampus (lower right) at indicated time intervals. (B) Representative ^{18}F-FDG PET coronal images superimposed on MR images between 45 and 90 minutes of the 2VGO (upper left panels) and 2VO (upper right panels) groups. Temporal profiles of the mean normalized ^{18}F-FDG count between 45 and 90 minutes in the cerebral cortex (lower left), caudoputamen (lower middle), and hippocampus (lower right) at indicated time intervals. Three to 4 animals in each group were used at each point. * $p < 0.05$; ** $p < 0.01$, 2VGO vs. 2VO. † $p < 0.05$, †† $p < 0.01$, at each period in 2VO group versus preoperation.

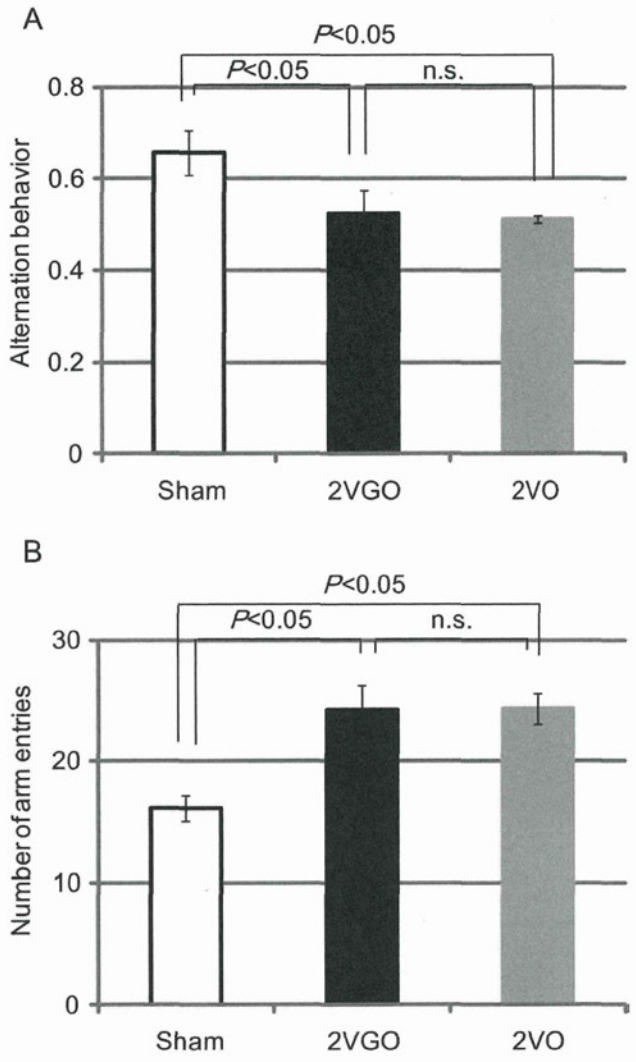

Fig. 6. Histogram showing spatial working memory impairment (A) and the locomotor activity (B) measured by Y-maze test at 28 days postoperation in the sham ($n = 10$), 2-vessel gradual occlusion (2VGO) ($n = 11$) and 2-vessel occlusion (2VO) ($n = 10$) groups.

density of GST-π-positive oligodendrocytes (Fig. 7C) were discovered: the white matter damage was slightly milder in the 2VGO compared with the 2VO groups but was still more severe than the sham group. In the 2VGO and 2VO groups, MAG-immunopositive regions (indicating the degree of axon-glial integrity) decreased compared with the sham group, with the most apparent difference at 28 days (data not shown). The density of glial fibrillary acidic protein-immunopositive astrocytes was significantly greater in both the 2VGO and 2VO groups compared with the sham group at 28 days (data not shown). The density of ionized calcium binding adapter molecule-1-immunopositive microglia increased from 1 day in the 2VO group; while in the 2VGO group, there was no change in microglia density at 1 day but an increase at 3 days. The microglial density in both the 2VGO and 2VO groups remained significantly greater than the sham group at 28 days (Supplemental Fig. 2A and B).

3.8. Western blotting analysis for MBP at 28 days postoperation

In addition to dMBP immunohistochemistry, MBP immunoblotting was evaluated as a marker of white matter integrity. Western blotting for MBP at 28 days showed multiple bands corresponding to the 4 isoforms (21.5/18.5/17/14 kDa). Densitometric analyses showed significant reduction in those bands both in the 2VGO and 2VO groups compared with the sham group. However, the reduction was less substantial in the 2VGO than 2VO groups (Fig. 8).

3.9. mRNA expression of inflammatory cytokines at 1 day postoperation

At 1 day, cerebral mRNA expression of inflammatory cytokines, MCP-1, and TNF-α was significantly increased in the 2VO group but slightly increased in the 2VGO group compared with the sham group (Fig. 9A and B).

3.10. The protein level of TNF-α at 1 day postoperation

At 1 day, cerebral protein level of TNF-α was significantly increased in both the 2VGO and 2VO groups compared with the sham group, with a tendency of increase in the 2VO group (Fig. 9C).

4. Discussion

The findings in this study suggest circumvention of the acute phase of CBF reduction and resultant acute inflammatory response observed in the 2VO model by gradual narrowing of the bilateral CCAs using the ameroid constrictor device instead of ligation. As a result, segregation of the chronic phase from the acute phase was achieved, suggesting a more precise reconstruction of chronic cerebral hypoperfusion evident in clinical cases of SIVD. This method induced demyelinating changes with inflammatory and glial responses but without apparent infarcted lesions or pronounced metabolic derangement in the gray matter. White matter changes were substantial in both the 2VGO and 2VO groups but significantly less severe in the 2VGO group. This suggests that the neuropathological consequences and metabolic changes of the 2VO model had been generated not only by chronic cerebral hypoperfusion but also by acute drop in CBF immediately after bilateral CCAs occlusion. The differences in mortality rate, infarction rate, and body weight loss between the 2VGO and 2VO groups may reflect gradual CBF reduction in the 2VGO group.

Y-maze tests showed significant spatial working memory impairment in both the 2VGO and 2VO groups. The spatial working memory impairment in the 2VGO model may be derived from white matter damage because neuropathological changes and glucose hypometabolism were not apparent in the cortex and hippocampus at 28 days. By contrast,

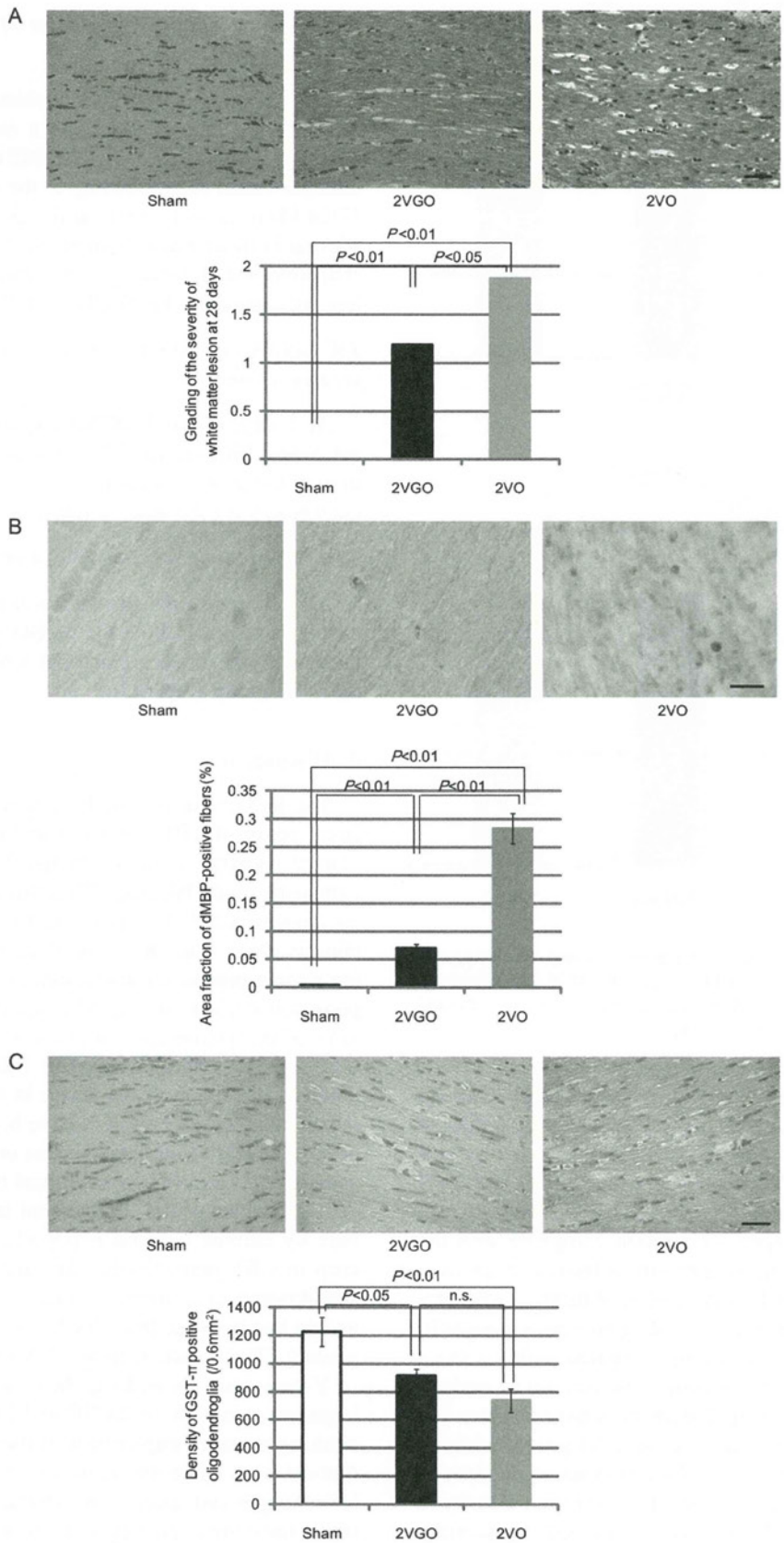
A
Sham
2VGO
2VO
P<0.01
P<0.01
P<0.05
Grading of the severity of white matter lesion at 28 days
2
1.5
1
0.5
0
Sham
2VGO
2VO
B
Sham
2VGO
2VO
P<0.01
P<0.01
P<0.01
Area fraction of dMBP-positive fibers (%)
0.35
0.3
0.25
0.2
0.15
0.1
0.05
0
Sham
2VGO
2VO
C
Sham
2VGO
2VO
P<0.01
P<0.05
n.s.
Density of GST-π positive oligodendroglia (/0.6mm²)
1400
1200
1000
800
600
400
200
0
Sham
2VGO
2VO

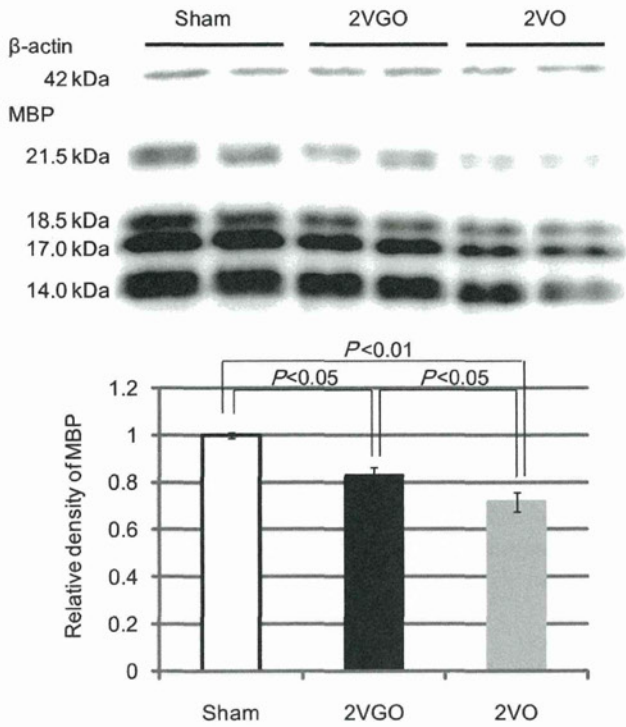

Fig. 8. Representative images of immunoblotting for myelin basic protein (MBP) and β-actin in the optic nerve and chiasma of the sham (n = 4), 2-vessel gradual occlusion (2VGO) (n = 4), and 2-vessel occlusion (2VO) (n = 4) groups at 28 days postoperation. Histogram showing the relative amount of MBP as assessed by densitometric analysis.

the 2VO model exhibited persistent metabolic derangement in the gray matter at 28 days, despite CBF recovery; this suggests neurovascular uncoupling even at 28 days postoperation. The 2VO and 2VGO model may thus be defined by the presence or absence of the acute CBF drop, respectively; therefore, the persistent neurovascular uncoupling at 28 days in the 2VO group may result from the ischemic insult applied to the brain in the acute phase postoperation. These results therefore suggest that the 2VGO model may more closely replicate the condition of working memory impairment subsequent to ischemic white matter changes.

The reasons as to why the 2VGO model showed comparable spatial working memory impairment to the 2VO model may be explained by the fact that less pronounced white matter damage was sustained in the 2VGO model compared with the 2VO model where the damage was sufficient to induce spatial working memory impairment detected by the Y-maze test. Another reason may be the impaired glial-axon integrity (assessed with MAG immunostaining) (Quarles, 2007), which was comparable between 2VGO and 2VO models; this therefore may have contributed to the working memory impairment.

No single animal model appears to recapitulate all the features of SIVD as humans have different brain anatomy and longer perforating arteries. In addition, the current model lacks vascular risk factors and causative small vessel changes that may lead to alterations in blood flow and cerebral autoregulation. One of the ways to resolve this problem could be to implant ameroid constrictors in spontaneous hypertensive rats (SHR) (Lin et al., 2001). However, SHRs subjected to the bilateral CCA occlusion have shown more extensive CBF reduction accompanied by more extensive cerebral infarcts and demyelinating changes and higher mortality rate (72%; 78 of 108) than the corresponding normotensive counterpart WKY rats (16%; 7 of 43) (Fujishima et al., 1976; Ogata et al., 1976). Besides the high mortality, such severe CBF reduction with marked infarctions may not adequately represent SIVD. Our preliminary data showed that the mortality rate of SHRs subjected to implantation of ameroid constrictors to the bilateral CCAs was only 6.2% (1 of 16) (Kitamura, unpublished data). Therefore, comparison of the effects of 2VGO on SHRs and on WKY rats could facilitate our understanding of the clinical and pathological substrates of SIVD with small vessel pathology, with the caveat that the genetic background of SHR is not necessarily identical to that of WKY rats (St. Lezin et al., 1992).

Thus far, rats with several different backgrounds have been used for 2VO model, including Sprague-Dawley, Wistar, and WKY rats. There may therefore have been discrepancies between rats in terms of the temporal CBF profile after 2VO. The relative CBF reduction from the baseline level in the current study was smaller than that found in Sprague-Dawley or Wistar rats but approximated that of WKY rats (Farkas et al., 2007).

The ameroid constrictor has been applied to the porcine or canine coronary arteries to simulate atherosclerotic coronary heart disease (Litvak et al., 1957), and the rabbit and rat femoral arteries to mimic chronic hind limb ischemia (Tang et al., 2005). However, this is the first report that the ameroid constrictor is applied to the CCA to replicate

Fig. 7. (A) Representative images of Klüver-Barrera staining in the corpus callosum at 28 days postoperation in each group (upper panels). Histogram showing the grading of the white matter lesions in the sham (n = 4), 2-vessel gradual occlusion (2VGO) (n = 4), and 2-vessel occlusion (2VO) (n = 4) groups. Scale bar, 50 μm. (B) Representative images of immunohistochemical staining for degraded myelin basic protein (dMBP) in the corpus callosum at 28 days in each group (upper panels). Oligodendrocytic cell bodies of irregular size and myelin sheaths along the axons were densely stained for dMBP. Scale bar, 20 μm. Histogram showing the area fraction (%) of dMBP-immunopositive fibers in the sham (n = 4), 2VGO (n = 4), and 2VO (n = 4) groups. (C) Representative images of the immunohistochemical staining for glutathione S-transferase-pi (GST-π) in the corpus callosum at 28 days in each group (upper panels). Histogram showing the density of GST-π-immunopositive oligodendroglia in the sham (n = 4), 2VGO (n = 4), and 2VO (n = 4) groups. Scale bar, 50 μm.

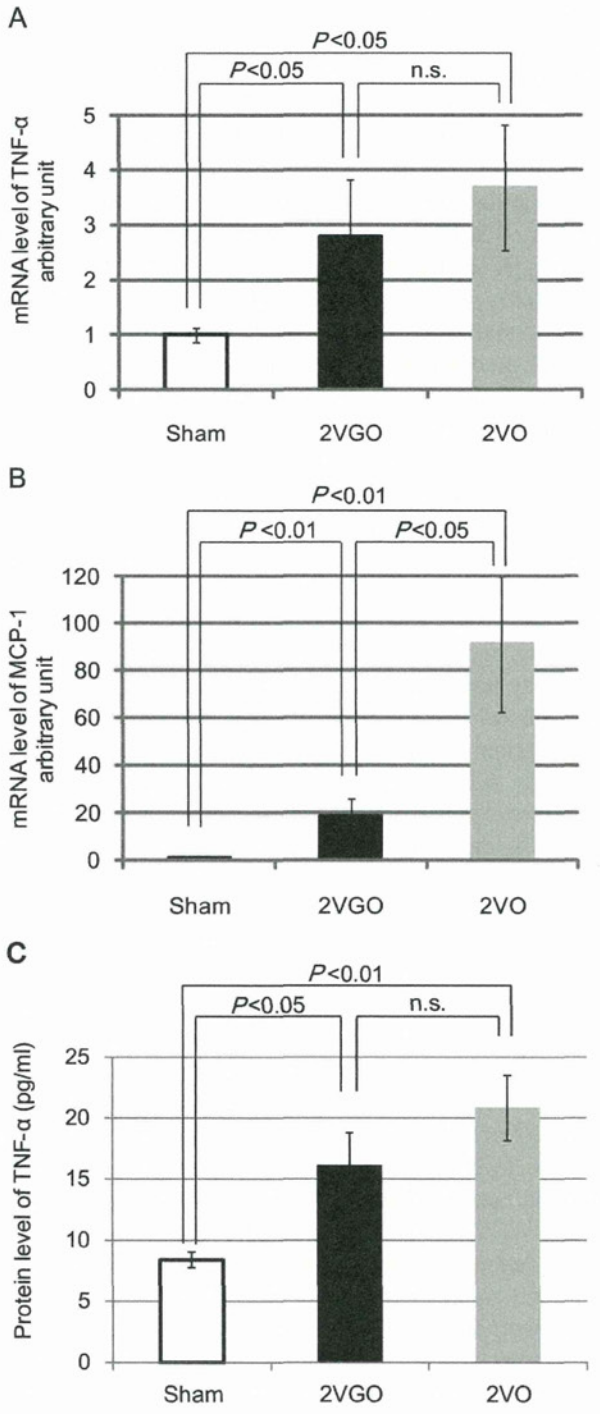

Fig. 9. Histogram showing the messenger RNA levels of tumor necrosis factor-α (TNF-α) (A) and monocyte chemoattractant protein-1 (MCP-1) (B), as analyzed with real-time reverse transcriptase-polymerase chain reaction (RT-PCR), in the right anterior hemisphere of the sham (normalized as 1), 2-vessel gradual occlusion (2VGO) (18.7 ± 7.28 and 2.79 ± 1.02 -fold, respectively), and 2-vessel occlusion (2VO) (91.2 ± 28.8 and 3.68 ± 1.14 -fold, respectively) groups at 1 day postoperation ($n = 4$ in each group). (C) Histogram showing the protein level of TNF-α, as analyzed with enzyme-linked immunosorbent assay (ELISA), in the left anterior hemisphere of the sham (8.38 ± 0.63), 2VGO (16.0 ± 2.70), and 2VO (20.8 ± 2.67) groups at 1 day postoperation ($n = 4$ in each group).

chronic cerebral hypoperfusion. Although the ameroid constrictor device achieves predictable gradual narrowing of the artery, the speed of arterial narrowing is dependent on both the size of ameroid constrictor and the diameter of arteries. As such, an in vivo noninvasive imaging technique, such as CTA, may be applicable in the evaluation of the temporal change in carotid blood flow. Moreover, use of titanium for casing, instead of the stainless steel, will enable magnetic resonance imaging/angiography.

Rats of 12–14 weeks of age were used in the current study to reproduce chronic cerebral hypoperfusion. However, application of the ameroid constrictor to older animals for longer periods should be considered given that SIVD is an age-related disease that develops over many years.

In conclusion, we have established a novel rat model that may more closely mimic cognitive impairment subsequent to selective white matter damage. The 2VGO model may therefore be adapted to explore possible treatments for SIVD.

Disclosure statement

The authors disclose no conflicts of interest.

All procedures were performed in accordance with the guidelines for animal experimentation from the ethical committee of Kyoto University.

Acknowledgements

We thank Dr. Matsuo and Dr. Wakita for generously giving us the anti-dMBP antibody, and Dr. Khundakar for insightful comments and editing. We are indebted to Ms. Tanigaki, Ms. Hikawa, Ms. Nakabayashi, Ms. Kawada, Ms. Katsukawa, and Mr. Kubota for their excellent technical assistance. This work was supported by grants from the Suzuken Memorial Foundation (to MI and JT) and the Japanese Vascular Disease Research Foundation (MI). The research work of R.N.K. is supported by the Medical Research Council, UK.

Appendix A. Supplementary data

Supplementary data associated with this article can be found, in the online version, at doi:10.1016/j.neurobiolaging.2011.10.033.

References

Farkas, E., Luiten, P.G., Bari, F., 2007. Permanent, bilateral common carotid artery occlusion in the rat: a model for chronic cerebral hypoperfusion-related neurodegenerative diseases. Brain Res. Rev. 54, 162–180.

Fujishima, M., Ogata, J., Sugi, T., Omae, T., 1976. Mortality and cerebral metabolism after bilateral carotid artery ligation in normotensive and spontaneously hypertensive rats. J. Neurol. Neurosurg. Psychiatry 39, 212–217.

Hainsworth, A.H., Markus, H.S., 2008. Do in vivo experimental models reflect human cerebral small vessel disease? A systematic review. J. Cereb. Blood Flow Metab. 28, 1877–1891.

Ihara, M., Polvikoski, T.M., Hall, R., Slade, J.Y., Perry, R.H., Oakley, A.E., Englund, E., O'Brien, J.T., Ince, P.G., Kalaria, R.N., 2010. Quantification of myelin loss in frontal lobe white matter in vascular dementia, Alzheimer's disease, and dementia with Lewy bodies. Acta Neuropathol. 119, 579–589.

Jiwa, N.S., Garrard, P., Hainsworth, A.H., 2010. Experimental models of vascular dementia and vascular cognitive impairment: a systematic review. J. Neurochem. 115, 814–28.

Lin, J.X., Tomimoto, H., Akiguchi, I., Wakita, H., Shibasaki, H., Horie, R., 2001. White matter lesions and alteration of vascular cell composition in the brain of spontaneously hypertensive rats. Neuroreport 12, 1835–1839.

Litvak, J., Siderides, L.E., Vineberg, A.M., 1957. The experimental production of coronary artery insufficiency and occlusion. Am. Heart J. 53, 505–518.

Marosi, M., Rákos, G., Robotka, H., Németh, H., Sas, K., Kis, Z., Farkas, T., Lür, G., Vécsei, L., Toldi, J., 2006. Hippocampal (CA1) activities in Wistar rats from different vendors. Fundamental differences in acute ischemia. J. Neurosci. Methods 156, 231–235.

Marshall, R.S., Lazar, R.M., 2011. Pumps, aqueducts, and drought management: vascular physiology in vascular cognitive impairment. Stroke 42, 221–226.

Ogata, J., Fujishima, M., Morotomi, Y., Omae, T., 1976. Cerebral infarction following bilateral carotid artery ligation in normotensive and spontaneously hypertensive rats: a pathological study. Stroke 7, 54–60.

Otori, T., Katsumata, T., Muramatsu, H., Kashiwagi, F., Katayama, Y., Terashi, A., 2003. Long-term measurement of cerebral blood flow and metabolism in a rat chronic hypoperfusion model. Clin. Exp. Pharmacol. Physiol. 30, 266–272.

Pantoni, L., 2010. Cerebral small vessel disease: from pathogenesis and clinical characteristics to therapeutic challenges. Lancet Neurol. 9, 689–701.

Quarles, R.H., 2007. Myelin-associated glycoprotein (MAG): past, present and beyond. J. Neurochem. 100, 1431–1448.

Shibata, M., Ohtani, R., Ihara, M., Tomimoto, H., 2004. White matter lesions and glial activation in a novel mouse model of chronic cerebral hypoperfusion. Stroke 35, 2598–2603.

St. Lezin, E., Simonet, L., Pravenec, M., Kurtz, T.W., 1992. Hypertensive strains and normotensive "control" strains. How closely are they related? Hypertension 19, 419–424.

Tang, G.L., Chang, D.S., Sarkar, R., Wang, R., Messina, L.M., 2005. The effect of gradual or acute arterial occlusion on skeletal muscle blood flow, arteriogenesis, and inflammation in rat hindlimb ischemia. J. Vasc. Surg. 41, 312–320.

Tomimoto, H., Ihara, M., Wakita, H., Ohtani, R., Lin, J.X., Akiguchi, I., Kinoshita, M., Shibasaki, H., 2003. Chronic cerebral hypoperfusion induces white matter lesions and loss of oligodendroglia with DNA fragmentation in the rat. Acta Neuropathol. 106, 527–534.

Wakita, H., Tomimoto, H., Akiguchi, I., Kimura, J., 1994. Glial activation and white matter changes in the rat brain induced by chronic cerebral hypoperfusion: an immunohistochemical study. Acta Neuropathol. 87, 484–492.

Wakita, H., Tomimoto, H., Akiguchi, I., Matsuo, A., Lin, J.X., Ihara, M., McGeer, P.L., 2002. Axonal damage and demyelination in the white matter after chronic cerebral hypoperfusion in the rat. Brain Res. 924, 63–70.

Yoshitake, T., Kiyohara, Y., Kato, I., Ohmura, T., Iwamoto, H., Nakayama, K., Ohmori, S., Nomiyama, K., Kawano, H., Ueda, K., et al., 1995. Incidence and risk factors of vascular dementia and Alzheimer's disease in a defined elderly Japanese population: the Hisayama Study. Neurology 45, 1161–1168.

Yoshizaki, K., Adachi, K., Kataoka, S., Watanabe, A., Tabira, T., Takahashi, K., Wakita, H., 2008. Chronic cerebral hypoperfusion induced by right unilateral common carotid artery occlusion causes delayed white matter lesions and cognitive impairment in adult mice. Exp. Neurol. 210, 585–591.

Journal of the Neurological Sciences 322 (2012) 141–147

Contents lists available at SciVerse ScienceDirect

Journal of the Neurological Sciences

journal homepage: www.elsevier.com/locate/jns

Does vascular pathology contribute to Alzheimer changes?

Raj N. Kalaria *, Rufus Akinyemi, Masafumi Ihara

Centre for Brain Ageing and Vitality, Institute for Ageing and Health, Newcastle University, Campus for Ageing & Vitality, Newcastle Upon Tyne NE4 5PL, United Kingdom
Department of Neurology, Kyoto University Graduate School of Medicine, 54 Kawaharacho, Shogoin, Sakyo, Kyoto 606-8507, Japan

ARTICLE INFO

Article history:
Received 23 February 2012
Received in revised form 10 July 2012
Accepted 11 July 2012
Available online 11 August 2012

Keywords:
Ageing
Alzheimer's disease
Dementia
Diabetes
Diet
Hypertension
Physical activity
Stroke
Vascular dementia
White matter lesions

ABSTRACT

In recent years there has been increased interest in whether vascular disease contributes to Alzheimer's disease (AD). This review considers how modifiable risk factors such as hypertension, atherosclerosis, diabetes, dyslipidaemia and adiposity may impact on vascular structure and function to promote neurodegenerative processes and instigate AD. The presence of vascular pathology involving arterial stiffness, arteriolosclerosis, endothelial degeneration and blood–brain barrier dysfunction leads to chronic cerebral hypoperfusion. Pathological changes in human brain and animal studies suggest cerebral hypoperfusion which in turn induces several features of AD pathology including selective brain atrophy, white matter changes and accumulation of abnormal proteins such as amyloid β. Cerebral pathological changes may be further modified by genetic factors such as the apoliopoprotein E ε4 allele. Although tau hyperphosphorylation and tangle formation still needs robust explanation further support for the notion that vascular pathology influences AD changes is provided by the evidence that interventions which improve vascular function attenuate AD pathology.

1. Introduction

Epidemiological, clinicopathological and animal studies show that both systemic vascular disorders and cerebrovascular disease (CVD) in various forms contribute to cognitive decline [1]. Increasing age is the strongest risk for dementia whether it results from a vascular aetiology or neurodegenerative disease processes such as in Alzheimer's disease (AD). Age is the overarching common factor when considering the impact of one type of pathology on the other which results in single or additive effects on dementia. AD and vascular dementia (VaD) or vascular cognitive impairment (VCI), the two most common causes of dementia, represent two extremes of the spectrum, and in-between entities with varying degrees of neurodegenerative and vascular pathologies occur. These entities include AD with cerebrovascular disease (mixed dementia), AD with vascular lesions, AD with severe cerebral amyloid angiopathy (CAA), CAA with plaques, VCI with AD changes and VCI with small vessel disease (SVD) [2] but are more common than the 'pure' conditions of AD and VaD. The pure forms are preferred for convenience to label, treat or manage but conditions within the spectrum are the norm rather than the exception. The greater degree of one type pathology over another may inform on the interactions between different pathologies. Here, we review evidence from relevant human and animal studies for the contribution or influence of vascular changes on the development and progression of the pathological features which characterise AD. The information also demonstrates that vascular disease triggers or uncovers dementia but the types invariably include AD.

2. Vascular disease as risk factor for increasing clinically diagnosed AD

Several vascular risk factors have been found to be associated with AD type of dementia. These include hypertension, diabetes mellitus, atherosclerosis, hypercholesterolemia, obesity and metabolic syndrome, smoking and certain forms of coronary disease (Table 1). Transient ischemic attacks and stroke episodes as indicators of large or small vessel disease also increase incidence of AD. The apolipoprotein E (ApoE; *APOE*) genotype with the link to dynamics of cholesterol transport is also implicated as a vascular risk factor in influencing AD. Among the vascular disease factors hypertension appears to be the strongest risk for AD [3]. Most studies demonstrate that hypertension in mid-life predisposes to cognitive decline and AD type of dementia in late life [4,5], although a few studies have found negative or no correlation [6–8]. Several reasons including low statistical power may explain the lack of association in these studies. However, long-standing increase in blood pressure may increase risk of dementia by inducing small vessel disease, white matter (WM) changes and cerebral hypoperfusion through the disruption of

* Corresponding author at: Institute for Ageing and Health, Campus for Ageing & Vitality, Newcastle Upon Tyne, NE4 5PL, United Kingdom. Tel.: +44 191 248 1352; fax: +44 191 248 1301.
E-mail address: raj.kalaria@ncl.ac.uk (R.N. Kalaria).

0022-510X/$ – see front matter © 2012 Elsevier B.V. All rights reserved.
doi:10.1016/j.jns.2012.07.032

Table 1
Vascular risk factors for Dementia and AD.
Data from several references [4,5,15,20,27,30,90].

Type of risk	Individual features	Times relative risk*	Pathological verification
Stroke(s)/vascular origin	Silent infarcts	1.2	N/A
	Stroke	3	Yes
	Transient ischaemic attacks	2	–
Vascular pathology: atherosclerosis	Carotid arteries	2	–
	Aortic arch	2	Yes
	Circle of Willis	2	Yes
Blood pressure	Hypertension systolic BP; >130 mm Hg; diastolic>95 mm Hg	2–3	Yes
Heart disease	Coronary artery disease	2	Yes
	Atrial fibrillation	2	No
Diabetes	Type I	1.3	No
	Type II	1.4	Yes, NFT increased
Dyslipidemia	High cholesterol	1.5	No
	High triglycerides	1.5	No
Homocysteine	Hyperhomocysteinemia; >13 mmol	2	No

This table lists factors that may directly or indirectly affect vascular health. *Degree of risk (strong means>3 fold RR or HR; weak means<two-fold RR or HR) were derived from published relative risk (RR) and hazard ratios (HR).

vasoregulatory functions or atherosclerotic disease [9]. Antihypertensive therapies have been shown to decrease the incidence of cognitive decline and dementia [10] and reduce AD pathology [11].

The increased risk of dementia in diabetes mellitus (DM) is attributed to CVD [12,13] and the association of AD with DM is clearer when milder cases are included in the analysis [14]. DM causes ischaemic CVD, primarily lacunar infarcts, and is positively associated with AD pathology through hyperinsulinemia (causing increased secretion but reduced extracellular degradation of amyloid β), impaired insulin signalling, oxidative stress, inflammatory mechanisms and coupling of neuronal components by advanced glycation end products [15]. Individuals with high BMIs have a significantly greater risk of dementia [16] whereas those who were obese at mid-life have a 3-fold increased risk of dementia (AD, VaD) in old age [17]. Hypercholesterolemia in mid-life also tends to show positive association with dementia including AD and VaD [18–20] although cholesterol levels assessed in late life reveal less significant association with AD [21,22]. Statins have a broad range of properties including antioxidant activity, immunomodulation and regulation of inflammatory processes, all of which could prevent neuronal death and generally exhibit beneficial effects. Simvastatin has been found to reduce the levels of amyloid β peptides (Aβ42 and Aβ40) [23], but the results of clinical studies do not consistently show robust protective effects of statins in preventing AD [24].

Smoking predisposes to oxidative stress, atherosclerosis, plaque formation and silent brain infarctions . In the Honolulu-Asia Ageing Study (HAAS), the association between mid-life smoking and late-life dementia, following adjustment for age, education and *APOE* genotype, showed the risk of AD in smokers increased with pack-years of smoking. Neuropathological findings in a sub-sample showed increased number of neuritic plaques with higher smoking levels [25]. Another study has also demonstrated that heavy smoking in mid-life is associated with >100% increased risk of AD and VaD after over twenty years [26].

Atherosclerosis predisposes to small and large infarcts and cerebral hypoperfusion leading to vascular and degenerative changes associated with cognitive decline and both AD and VaD. Other complications relating to atherosclerosis include coronary heart disease and congestive heart failure. The Rotterdam study revealed that atherosclerosis, predominantly of the carotid arteries, was associated with an increased risk of dementia [AD and VaD] [27]. A significant association between coronary disease and dementia, and AD through the causation of multiple cerebral emboli and reduced cerebral perfusion has also been reported [28,29]. Although homocysteine is an established risk factor for cardiovascular disease, its role in dementia has been controversial [30]. High homocysteine concentrations in mid-life is an independent risk factor for the development of late-life AD in women [31]. Although these epidemiological studies do not explain how pre-existing or co-morbid vascular disease precisely impacts on processes that lead to neurodegeneration characteristic of AD they collectively demonstrate that there is a clear link between vascular disease and an increased burden of AD (Table 2). Furthermore, a Rottterdam study demonstrated that silent brain infarcts detected on magnetic resonance (MR) imaging doubled the risk of dementia and AD in elderly community-dwellers [32] Thus a number of vascular disease risk factors indicate greater or cumulative risk of AD primarily via a vascular effect rather than distinctive neuronal degeneration (Fig. 1).

3. Influence of Apolipoprotein E (Apo E)

ApoE is a major constituent of very low density lipoproteins (VLDL) and plays a key role in the transport of cholesterol among various cells of the body. *APOE* ε4 allele is associated with younger onset AD, and increases disease risk in a dose-dependent manner in both AD and VaD. *APOE* ε4 allele has the most consistent but varying modulating influence on the vascular factors, particularly blood pressure, diabetes, dyslipidaemia, atherosclerosis, lacunar infarcts and homocysteine [2,19]. Furthermore, the *APOE* ε4 allele may mediate risk for AD by decreasing resting CBF well before the onset of dementia [33].

4. Cerebrovascular pathology in AD

As implied above, AD and VaD to varying degrees demonstrate similarities in risk factors, pathophysiology and neuropathological substrates [2]. In the very first documented case of AD reported by Alzheimer, the

Table 2
Alzheimer type of changes in VaD.
Data taken from several original references cited in [12,58].

AD feature	Change and localization
CAA	Presence in cortical cerebral vessels
Amyloid peptides	Increased in temporal and frontal lobes
Tau isoforms (hyperphosphorylated)	Increased in CSF
Cholinergic neuronal markers	Decreased ChAT activity
Serotonergic markers	Decreased 5-HT concentrations
Synaptophysin	Decreased cortical activity
APOE ε4 allele	Presence in most VaD cases

This table lists overlap of markers linked to Alzheimer pathology present in VaD subjects.

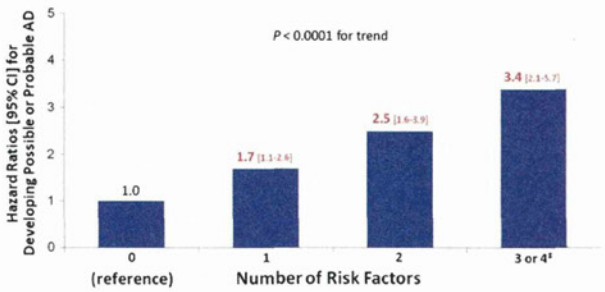

Fig. 1. Graph shows cumulative risk for probable and possible AD. In this study 1138 individuals without dementia were screened at baseline. The risk factors included diabetes, hypertension, heart disease and smoking. Heart disease was indicated by history of atrial fibrillation and other arrhythmias, myocardial infarction, congestive heart failure and angina pectoris.
Data modified from Luchsinger J et al. [91].

descriptions of autopsy findings in the index patient, showed considerable microvascular pathology [34]. Several autopsy series have reported the existence of a high degree of vascular pathology. From 60 to 90% of AD patients exhibit various cerebrovascular pathologies including white matter lesions, CAA, microinfarcts, small infarcts, haemorrhages and microvascular degeneration [2,35–39]. It is also recognized that with co-existent pathological substrates of AD and cerebrovascular lesions, it takes lower burden of AD pathology to produce the same degree of dementia [40]. The Nun Study showed that individuals with one or two lacunar infarcts have a steeper drop in cognitive function compared to those with no infarcts [41]. While the relationship between AD pathology and infarctions is debated the presence of one or more infarctions independently increases the odds of dementia beyond their additive effect [42]. Periventricular lesions and cerebral microbleeds [43] are also associated with degenerative pathology [44].

5. White matter changes and AD pathology

White matter changes reflected by white matter hyperintensities (WMHs), lacunar infarcts, enlarged Virchow Robin spaces and microbleeds upon MR imaging are often present to a variable degree in clinically diagnosed AD. Using positron emission tomography imaging, WMHs correspond to areas of hypometabolism, reduced CBF and increased oxygen extraction which are further evidence of the ischaemic origin [45,46] but evident in AD. Frontal WMHs scored upon imaging were associated with increasing burden of neurodegenerative pathology as determined by Braak staging [38,47].

Neuropathological findings suggest that demyelination evolves in parallel with shrunken oligodendrocytes in VaD but their increased density in AD [38], while these observations highlight partially different mechanisms associated with myelin degeneration both could originate from chronic hypoxic damage to oligodendrocytes and other components of the WM [48]. However, myelin loss secondary to axonal degeneration in AD cannot be excluded. Imaging studies also suggest breach of the BBB especially in those subjects with history of vascular disease irrespective of type of clinical diagnosis of dementia type [49].

6. Vascular basis of the neurovascular unit

The 'neurovascular unit' describes a close developmental, structural and functional relationship existing among the cerebral microvascular cells (endothelium, pericytes and adventitial cells), neurons and glial cells (astrocytes, microglia and oligodendrocytes). This relationship, 'neurovascular coupling' ensures a coordinated response to injury to any of the component parts of the unit that may be vulnerable to amyloid [50]. To maintain the integrity of the neurovascular unit, certain cerebrovascular mechanisms are in place which include cerebrovascular autoregulation, functional hyperaemia and the blood brain barrier (BBB) [51,52]. Cerebrovascular autoregulation ensures that cerebral blood flow (CBF) is maintained independently of alterations in mean arterial blood pressure while functional hyperaemia ensures that blood flow is increased to an activated brain region through the release of several vasoactive agents (including nitric oxide, prostanoids, adenosine, K+ ions, carbon monoxide, cytochrome p450 metabolites) from neurons, astrocytes and vascular cells. The BBB limits the entry of potentially toxic substances into the brain through its impermeable membrane [52,53].

Cerebrovascular disease and systemic vascular disorders may irreversibly affect these defence mechanisms leading to reduction of regional blood flow and loss of autoregulation causing cerebral hypoperfusion (Fig. 2). Previous observations in biopsy cortical tissue from AD subjects has indicated various features consistent with BBB breakdown [51]. These include thinning of the endothelium, loss of mitochondria and thickening of basement membranes, which increase focal amyloid β peptides accumulation. A breach of the BBB also leads to potentially toxic substances and metabolites gaining access into the brain [52,53].

7. How might cerebrovascular disease affect the neurovascular unit and produce AD changes?

The structural and functional changes associated with CVD will cause a reduction in CBF at rest and during brain activation. It has been hypothesised that when this reduction reaches a critical level, described as the "Critically Attained Threshold of Cerebral Hypoperfusion (CATCH)"

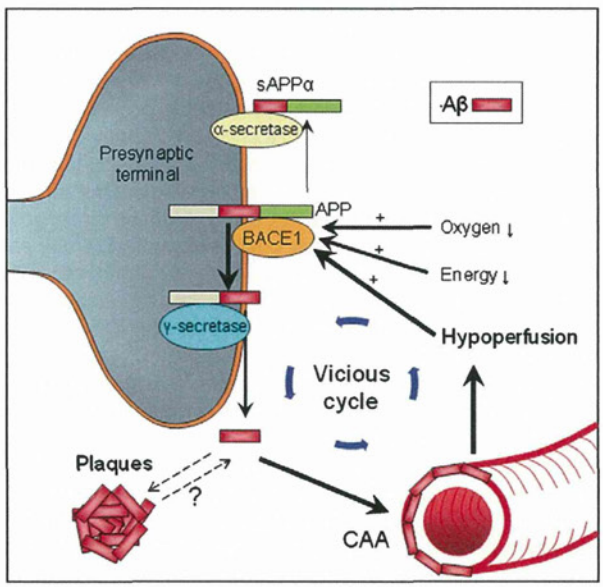

Fig. 2. Vascular changes may influence Alzheimer lesion burden: evidence from animal studies. Scheme and arrows indicate how cerebrovascular factors affect the amyloid β processing and clearance. (1) When oxygen is in short supply as a result of arteriolosclerosis or blood–brain barrier (BBB) disruption, hypoxia-inducible factor (HIF)-1α is induced, which binds to the hypoxia-responsive element (HRE) on the β amyloid cleaving enzyme 1 (BACE1) promoter region and upregulates the expression of BACE1 mRNA, subsequently leading to predominant generation of amyloid β over secreted (s) amyloid precursor protein α. (2) The energy insufficiency, which could result from hypoperfusion, elevates BACE1 levels and activity, leading to amyloid β overproduction [92], probably through the stress-activated p38 pathway. (3) Chronic hypoperfusion itself (and the resultant energy and oxygen deficiency) also elevates BACE1 expression and amyloid β generation. (4) Amyloid β overproduction leads to amyloid plaque formation and cerebral amyloid angiopathy (CAA). (5) CAA further potentiates deficiencies of oxygen, energy, and blood flow by aggravating preexisting arteriosclerosis and BBB disruption, thus forming the vicious cycle.

hypothesis [54], there is breakdown of the cerebrovascular defence system, arterial stiffness, uncoupling of the neurovascular unit, reduced clearance of by-products of brain activity, accumulation of such substances as amyloid β and activation of neuroinflammatory responses. Few longitudinal studies followed to autopsy support the thesis that hypoxia or oligaemia increases accumulation of AD pathological changes and cognitive dysfunction. Roher and colleagues [55–57] have shown that atherosclerotic occlusion of the circle of Willis arteries was more extensive in the AD subjects accompanied by a greater burden of neurofibrillary pathology and white matter rarefaction than in the non-demented ageing individuals but not against subjects with VaD. These observations were not necessarily influenced by the presence of an *APOE* ε4 allele, however. This and our previous autopsy findings [58] suggest that atherosclerosis-induced brain hypoperfusion contributes to the clinical and pathological manifestations of AD. In the Honolulu Heart Program/Honolulu-Asia ageing Study (HHP/HAAS) cohort elevated systolic BP (≥160 mm Hg) in midlife was associated with low brain weight and greater numbers of NP in both neocortex and hippocampus. Furthermore, diastolic BP elevation (≥95 mm Hg) was associated with greater numbers of NFT in the hippocampus. It is plausible that gradual arteriolosclerosis induces NFT formation in closely perfusing neuronal populations. However, these findings suggest that in addition to the accepted association of high BP with cerebrovascular lesions, there is a direct relationship with brain atrophy, neuritic plaques and neurofibrillary tangles [59].

Cerebral hypoperfusion or oligaemia induced by CVD may either initiate and/or accelerate the neurodegeneration cascade causing amyloid deposition, synaptic and neuronal dysfunction and lead to cognitive impairment [58] apart from the direct cognitive effect of microvascular pathology as seen in subjects with DM type II and AD [12]. As part of the compromise of cerebrovascular defence mechanisms occasioned by CVD, there could be disruption of the endothelium and the BBB causing transport disequilibrium across the barrier. However, the presence of brain microvessels within or juxtaposed to plaques in AD [60] also suggests the perfusing surface of the brain has a role in cerebral amyloidosis [9]. Cortical microvascular abnormalities may be impacted by ageing per se but greater degenerative changes are accelerated by amyloid deposition. Consistent with this, a recent study in rhesus monkeys [61] demonstrated that β amyloid cleaving enzyme 1 (BACE1)-labelled dystrophic axons resided near to or in direct contact with cortical blood vessels. Thus plaque formation in AD appears linked to a multisystem axonal pathogenesis occurring in partnership with potential vascular deficits (Fig. 2). This also explains why senile plaques preferentially occur near the cerebral microvasculature [62]. It is plausible that ageing associated microvascular abnormalities including disruption of the vascular extracellular matrix forms a nidus for amyloid β deposition [60].

Another vital mechanism by which CVD may cause cognitive impairment and Alzheimer type of dementia is through their impact on cholinergic neurotransmission which subserve a pivotal role in normal cognition, particularly in the domains of attention, emotion and memory [63]. CVD also impacts on the collections of cholinergic neurons in the basal forebrain including the nucleus basalis of Meynert (nBM). Ischaemic injury resulting from cerebral hypoperfusion leads to widespread disconnection of cholinergic innervations from the neuronal population of the nBM to other parts of the brain including the neocortex, and this has been documented in both AD and VaD [63,64].

Oxidative stress in the brain and cerebral blood vessels has been found to play a critical role in the processes associated with cerebrovascular dysfunction, with NADPH oxidase being a major source of reactive oxygen species (ROS) involved [50,65,66]. ROS alter vascular regulation through processes involving the formation of peroxynitrite from the reaction between nitric oxide (NO) and superoxide radical. Oxidative stress and reactive oxygen species resulting from mitochondrial dysfunction have, consequently, been strongly implicated in brain ageing, AD and VaD [67,68]. Overall, various factors may contribute to a chronic hypoperfusive state leading to microscopic tissue damage and regional specific syndromes (Fig. 2).

8. Ageing related vascular changes may impede clearance of proteins contributing to AD pathology

Increasing age is associated with structural changes and stiffness of the vasculature resulting in reduced tone and transport functions [51]. It has been previously suggested that age-related basement membrane thickening and loss of elasticity within the arterial vessels may reduce the amplitude of the pulsations, which is the main driving force for drainage of soluble proteins along the lymphatic drainage pathways. The deposition of amyloid β in the walls of arteries as CAA and impedance of perivascular drainage of amyloid β can have major consequences including intracerebral haemorrhage associated with rupture of amyloid β-laden arteries and further increase the burden of AD pathology [69,70]. Furthermore, the reduced expression of the low density lipoprotein receptor related protein (LRP) as a major efflux transporter and abnormalities in other transporters e.g. the advanced glycation end product receptor (RAGE) [71] in ageing rodents, non-human primates and AD patients [72,73] handling amyloid β peptides across a defective BBB would compromise the homeostasis of the cerebral microenvironment and increase oxidative and nitrosative damage as well as protease activity (Fig. 2).

9. Cerebral perfusion protects against AD type of pathology

The link between hypoxia or oligaemia and AD features e.g. region specific atrophy, accumulation of amyloid β and cognitive dysfunction has been difficult to readily address in man. We previously showed the differential but increased deposition of soluble amyloid β, particularly amyloid β(42) residue peptide in temporal and frontal lobes of VaD subjects compared to cognitively normal ageing individuals [44]. This suggests that stroke injury or oligaemia per se increases amyloid β accumulation although it may not be evident within visible neuritic plaques. Similarly, medial temporal atrophy (indicative of degenerative pathology) rather than WMHs (indicative of SVD) predicted cognitive decline and progressive brain atrophy in stroke survivors. This suggested a greater role for Alzheimer pathology rather than vascular pathology in the evolution of delayed cognitive impairment after stroke [74]. However, our recent findings suggest a vascular basis for medial temporal atrophy too including hippocampal cell atrophy in humans [75,76] and in rodents [77].

Select animal models have provided clues whether vascular changes increase the burden of AD pathology. Working on the hypothesis that stroke injury may accelerate clinicopathological changes in AD [78], we have examined whether chronic cerebral hypoperfusion accelerated amyloid beta deposition in a variety of amyloid protein precursor transgenic (APP-Tg) mouse [79,80]. In animals subjected to bilateral common carotid artery stenosis using an established procedure using microcoils, we found that the white matter was not only rarefied with increased astrogliosis but both amyloid peptides accumulated in axons and in short- and long-term hypoperfused animals. Further fractionation of extracellular cortical tissue showed an increase of amyloid β fibrils supporting the notion that cerebral hypoperfusion induced amyloid β deposition in the intracellular compartment and, accelerate the pathological changes of AD [79]. In a subsequent study, we found that cerebral hypoperfusion significantly reduced the density of Nissl-stained neurons and silver-stained cored plaques in the hippocampus of APP-Tg mice but increased the amount of filter-trap amyloid β in the extracellular-enriched soluble brain fractions. These observations suggested an interaction between chronic cerebral hypoperfusion and APP overexpression in cognitive decline in mice through enhanced neuronal loss and altered amyloid β

metabolism [80]. APP overexpressing mice that predominantly exhibit CAA show that following chronic cerebral hypoperfusion there is accelerated deposition of leptomeningeal amyloid β and that impaired microvascular function due to perivascular amyloid β accumulation precipitates microinfarcts [81]. These animal studies support the hypothesis that vascular pathology influences changes characterised by AD.

Clinical and epidemiological studies have shown that relevant diet, healthy nutrition and adequate physical exercise are important non-pharmacological, lifestyle-related interventions that could help maintain normal vascular tone, adequate CBF and normal cognition during ageing. For example, the higher adherence to a Mediterranean-type diet, regular consumption of fish and diets rich in polyphenols are associated with slower cognitive decline, reduced risk of progression from mild cognitive impairment to AD, reduced risk of AD or decreased all-cause mortality in AD [82–85]. There is a large body of evidence on the beneficial effects of physical exercise on brain health across the life span and reducing the risk of dementia [86]. There are few pathological studies in man verifying that the burden of vascular pathology is reduced with such interventions but various animal models allow this to be tested albeit with limitations.

Studies in amyloid over-expressing transgenic mice have shown that enriched environment (increased exercise) is a useful intervention to ameliorate behavioural changes and AD type pathological changes in normal [87] and in high fat diet-induced aggravation of equivalent AD symptoms [88]. Consistent with this adults who engage in high intensity physical activity are less vulnerable to the pathological effects of an unhealthy diet, while those with mild cognitive impairment have the greatest benefit of a healthy diet in modulating CSF amyloid β(42) concentrations only when paired with high physical activity [89]. Thus, vascular protective factors may attenuate pathological processes that ultimately modify risk of AD.

10. Summary

In balance, majority of epidemiological studies support the view that vascular disease risk factors impact on neurodegenerative processes. There are several caveats in this working hypothesis including the role of vascular disease in hyperphosphorylation of tau and tangle formation but both clinicopathological and animals studies suggest there is a strong link between vascular disease and Alzheimer-like changes if not AD per se. Almost all studies suggest vascular insufficiency or chronic cerebral hypoperfusion including that resulting from abnormalities within components of the neurovascular unit, increases white matter changes, axonal damage and cerebral amyloid deposition which may lead to atrophy. There is also evidence that interventions which improve vascular function attenuate AD pathology. Although there may not be a direct interaction between the two concomitant pathologies, vascular lesions in the presence of AD changes unquestionably worsens cognitive outcomes.

List of abbreviations

AD	Alzheimer's disease
CBF	cerebral blood flow
DM	diabetes mellitus
MRI	magnetic resonance imaging
ROS	reactive oxygen species
SVD	small vessel disease
VCI	vascular cognitive impairment
VaD	vascular dementia

Conflict of interest

None declared by the authors.

Acknowledgements

Our work has been supported by grants from the Medical Research Council (UK) for G0500247 and G0700718 awards, The CADASIL Trust (UK), US National Institutes of Health (NINDS) grant award NS054047 and the Alzheimer's Research Trust (UK). ROA was supported by an International Brain Research Organisation (IBRO) Research Fellowship.

References

[1] Gorelick PB, Scuteri A, Black SE, Decarli C, Greenberg SM, Iadecola C, et al. Vascular contributions to cognitive impairment and dementia: a statement for healthcare professionals from the American Heart Association/American Stroke Association. Stroke Sep 2011;42(9):2672-713.
[2] Kalaria RN. Similarities between Alzheimer's disease and vascular dementia. J Neurol Sci Nov 15 2002;203–204:29-34.
[3] Kennelly SP, Lawlor BA, Kenny RA. Blood pressure and the risk for dementia: a double edged sword. Ageing Res Rev Apr 2009;8(2):61-70.
[4] Skoog I, Lernfelt B, Landahl S, Palmertz B, Andreasson LA, Nilsson L, et al. 15-year longitudinal study of blood pressure and dementia. Lancet Apr 27 1996;347(9009):1141-5.
[5] Kivipelto M, Helkala EL, Laakso MP, Hanninen T, Hallikainen M, Alhainen K, et al. Midlife vascular risk factors and Alzheimer's disease in later life: longitudinal, population based study. BMJ Jun 16 2001;322(7300):1447-51.
[6] Farmer ME, White LR, Abbott RD, Kittner SJ, Kaplan E, Wolz MM, et al. Blood pressure and cognitive performance. The Framingham Study. Am J Epidemiol Dec 1987;126(6):1103-14.
[7] Verghese J, Lipton RB, Hall CB, Kuslansky G, Katz MJ. Low blood pressure and the risk of dementia in very old individuals. Neurology Dec 23 2003;61(12):1667-72.
[8] Morris MC, Scherr PA, Hebert LE, Glynn RJ, Bennett DA, Evans DA. Association of incident Alzheimer disease and blood pressure measured from 13 years before to 2 years after diagnosis in a large community study. Arch Neurol Oct 2001;58(10):1640-6.
[9] Kalaria RN. Vascular basis for brain degeneration: faltering controls and risk factors for dementia. Nutr Rev Dec 2010;68(Suppl. 2):S74-87.
[10] Takeda S, Sato N, Takeuchi D, Kurinami H, Shinohara M, Niisato K, et al. Angiotensin receptor blocker prevented beta-amyloid-induced cognitive impairment associated with recovery of neurovascular coupling. Hypertension Dec 2009;54(6):1345-52.
[11] Hoffman LB, Schmeidler J, Lesser GT, Beeri MS, Purohit DP, Grossman HT, et al. Less Alzheimer disease neuropathology in medicated hypertensive than nonhypertensive persons. Neurology May 19 2009;72(20):1720-6.
[12] Kalaria RN. Neurodegenerative disease: diabetes, microvascular pathology and Alzheimer disease. Nat Rev Neurol Jun 2009;5(6):305-6.
[13] Ahtiluoto S, Polvikoski T, Peltonen M, Solomon A, Tuomilehto J, Winblad B, et al. Diabetes, Alzheimer disease, and vascular dementia: a population-based neuropathologic study. Neurology Sep 28 2010;75(13):1195-202.
[14] Kopf D, Frolich L. Risk of incident Alzheimer's disease in diabetic patients: a systematic review of prospective trials. J Alzheimers Dis 2009;16(4):677-85.
[15] Luchsinger JA, Gustafson DR. Adiposity, type 2 diabetes, and Alzheimer's disease. J Alzheimers Dis Apr 2009;16(4):693-704.
[16] Whitmer RA, Gunderson EP, Barrett-Connor E, Quesenberry Jr CP, Yaffe K. Obesity in middle age and future risk of dementia: a 27 year longitudinal population based study. BMJ Jun 11 2005;330(7504):1360.
[17] Whitmer RA. The epidemiology of adiposity and dementia. Curr Alzheimer Res Apr 2007;4(2):117-22.
[18] Notkola IL, Sulkava R, Pekkanen J, Erkinjuntti T, Ehnholm C, Kivinen P, et al. Serum total cholesterol, apolipoprotein E epsilon 4 allele, and Alzheimer's disease. Neuroepidemiology 1998;17(1):14-20.
[19] Kivipelto M, Helkala EL, Laakso MP, Hanninen T, Hallikainen M, Alhainen K, et al. Apolipoprotein E epsilon4 allele, elevated midlife total cholesterol level, and high midlife systolic blood pressure are independent risk factors for late-life Alzheimer disease. Ann Intern Med Aug 6 2002;137(3):149-55.
[20] Solomon A, Kivipelto M, Wolozin B, Zhou J, Whitmer RA. Midlife serum cholesterol and increased risk of Alzheimer's and vascular dementia three decades later. Dement Geriatr Cogn Disord 2009;28(1):75-80.
[21] Tan ZS, Seshadri S, Beiser A, Wilson PW, Kiel DP, Tocco M, et al. Plasma total cholesterol level as a risk factor for Alzheimer disease: the Framingham Study. Arch Intern Med May 12 2003;163(9):1053-7.
[22] Reitz C, Tang MX, Luchsinger J, Mayeux R. Relation of plasma lipids to Alzheimer disease and vascular dementia. Arch Neurol May 2004;61(5):705-14.
[23] Fassbender K, Simons M, Bergmann C, Stroick M, Lutjohann D, Keller P, et al. Simvastatin strongly reduces levels of Alzheimer's disease beta-amyloid peptides Abeta 42 and Abeta 40 in vitro and in vivo. Proc Natl Acad Sci U S A May 8 2001;98(10):5856-61.
[24] McGuinness B, O'Hare J, Craig D, Bullock R, Malouf R, Passmore P. Statins for the treatment of dementia. Cochrane Database Syst Rev 2010(8):CD007514.
[25] Tyas SL, White LR, Petrovitch H, Webster Ross G, Foley DJ, Heimovitz HK, et al. Mid-life smoking and late-life dementia: the Honolulu-Asia Aging Study. Neurobiol Aging Jul–Aug 2003;24(4):589-96.
[26] Rusanen M, Rovio S, Ngandu T, Nissinen A, Tuomilehto J, Soininen H, et al. Midlife smoking, apolipoprotein E and risk of dementia and Alzheimer's disease: a population-based cardiovascular risk factors, aging and dementia study. Dement Geriatr Cogn Disord 2010;30(3):277-84.

[27] van Oijen M, de Jong FJ, Witteman JC, Hofman A, Koudstaal PJ, Breteler MM. Atherosclerosis and risk for dementia. Ann Neurol May 2007;61(5):403-10.
[28] Newman AB, Fitzpatrick AL, Lopez O, Jackson S, Lyketsos C, Jagust W, et al. Dementia and Alzheimer's disease incidence in relationship to cardiovascular disease in the Cardiovascular Health Study cohort. J Am Geriatr Soc Jul 2005;53(7):1101-7.
[29] Zuccala G, Onder G, Marzetti E, Monaco MR, Cesari M, Cocchi A, et al. Use of angiotensin-converting enzyme inhibitors and variations in cognitive performance among patients with heart failure. Eur Heart J Feb 2005;26(3):226-33.
[30] Seshadri S. Elevated plasma homocysteine levels: risk factor or risk marker for the development of dementia and Alzheimer's disease? J Alzheimers Dis Aug 2006;9(4):393-8.
[31] Zylberstein DE, Lissner L, Bjorkelund C, Mehlig K, Thelle DS, Gustafson D, et al. Midlife homocysteine and late-life dementia in women. A prospective population study. Neurobiol Aging Mar 31 2011;32:380-6.
[32] Ruitenberg A, den Heijer T, Bakker SL, van Swieten JC, Koudstaal PJ, Hofman A, et al. Cerebral hypoperfusion and clinical onset of dementia: the Rotterdam Study. Ann Neurol Jun 2005;57(6):789-94.
[33] Thambisetty M, Beason-Held L, An Y, Kraut MA, Resnick SM. APOE epsilon4 genotype and longitudinal changes in cerebral blood flow in normal aging. Arch Neurol 2010;67(1):93-8.
[34] Alzheimer A. Uber eine eigenartig Erkrankung er Hirnrinde. Allg Z Psychiat Psych-Gerichtl Med 1907;64:146-8.
[35] Premkumar DR, Cohen DL, Hedera P, Friedland RP, Kalaria RN. Apolipoprotein E-epsilon4 alleles in cerebral amyloid angiopathy and cerebrovascular pathology associated with Alzheimer's disease. Am J Pathol Jun 1996;148(6):2083-95.
[36] Kalaria RN, Ballard C. Overlap between pathology of Alzheimer disease and vascular dementia. Alzheimer Dis Assoc Disord Oct–Dec 1999;13(Suppl. 3):S115-23.
[37] Brun A, Englund E. A white matter disorder in dementia of the Alzheimer type: a pathoanatomical study. Ann Neurol Mar 1986;19(3):253-62.
[38] Ihara M, Polvikoski TM, Hall R, Slade JY, Perry RH, Oakley AE, et al. Quantification of myelin loss in frontal lobe white matter in vascular dementia, Alzheimer's disease, and dementia with Lewy bodies. Acta Neuropathol May 2010;119(5):579-89.
[39] Deramecourt V, Slade JS, Oakley AE, Perry RH, Ince PG, Maurage CA, Kalaria RN. Staging and natural history of cerebrovascular pathology in dementia. Neurology April 2012;78:1043-50.
[40] Riekse RG, Leverenz JB, McCormick W, Bowen JD, Teri L, Nochlin D, et al. Effect of vascular lesions on cognition in Alzheimer's disease: a community-based study. J Am Geriatr Soc Sep 2004;52(9):1442-8.
[41] Snowdon DA, Greiner LH, Mortimer JA, Riley KP, Greiner PA, Markesbery WR. Brain infarction and the clinical expression of Alzheimer disease. The Nun Study. JAMA Mar 12 1997;277(10):813-7.
[42] Schneider JA, Wilson RS, Bienias JL, Evans DA, Bennett DA. Cerebral infarctions and the likelihood of dementia from Alzheimer disease pathology. Neurology Apr 13 2004;62(7):1148-55.
[43] Qiu C, Winblad B, Fratiglioni L. The age-dependent relation of blood pressure to cognitive function and dementia. Lancet Neurol Aug 2005;4(8):487-99.
[44] Lewis H, Beher D, Cookson N, Oakley A, Piggott M, Morris CM, et al. Quantification of Alzheimer pathology in ageing and dementia: age-related accumulation of amyloid-beta(42) peptide in vascular dementia. Neuropathol Appl Neurobiol Apr 2006;32(2):103-18.
[45] Yamaji S, Ishii K, Sasaki M, Imamura T, Kitagaki H, Sakamoto S, et al. Changes in cerebral blood flow and oxygen metabolism related to magnetic resonance imaging white matter hyperintensities in Alzheimer's disease. J Nucl Med Sep 1997;38(9):1471-4.
[46] Takahashi W, Takagi S, Ide M, Shohtsu A, Shinohara Y. Reduced cerebral glucose metabolism in subjects with incidental hyperintensities on magnetic resonance imaging. J Neurol Sci May 1 2000;176(1):21-7.
[47] Polvikoski TM, van Straaten EC, Barkhof F, Sulkava R, Aronen HJ, Niinisto L, et al. Frontal lobe white matter hyperintensities and neurofibrillary pathology in the oldest old. Neurology Dec 7 2010;75(23):2071-8.
[48] Fernando MS, Simpson JE, Matthews F, Brayne C, Lewis CE, Barber R, et al. White matter lesions in an unselected cohort of the elderly: molecular pathology suggests origin from chronic hypoperfusion injury. Stroke Jun 2006;37(6):1391-8.
[49] Farrall AJ, Wardlaw JM. Blood–brain barrier: ageing and microvascular disease—systematic review and meta-analysis. Neurobiol Aging Mar 2009;30(3):337-52.
[50] Iadecola C. Neurovascular regulation in the normal brain and in Alzheimer's disease. Nat Rev Neurosci May 2004;5(5):347-60.
[51] Kalaria RN. Cerebral vessels in ageing and Alzheimer's disease. Pharmacol Ther 1996;72(3):193-214.
[52] Bell RD, Zlokovic BV. Neurovascular mechanisms and blood–brain barrier disorder in Alzheimer's disease. Acta Neuropathol Jul 2009;118(1):103-13.
[53] Iadecola C, Nedergaard M. Glial regulation of the cerebral microvasculature. Nat Neurosci Nov 2007;10(11):1369-76.
[54] de la Torre JC. Alzheimer disease as a vascular disorder: nosological evidence. Stroke Apr 2002;33(4):1152-62.
[55] Roher AE, Esh C, Kokjohn TA, Kalback W, Luehrs DC, Seward JD, et al. Circle of Willis atherosclerosis is a risk factor for sporadic Alzheimer's disease. Arterioscler Thromb Vasc Biol Nov 1 2003;23(11):2055-62.
[56] Roher AE, Tyas SL, Maarouf CL, Daugs ID, Kokjohn TA, Emmerling MR, et al. Intracranial atherosclerosis as a contributing factor to Alzheimer's disease dementia. Alzheimers Dement Mar 2011;7:436-44.
[57] Beach TG, Wilson JR, Sue LI, Newell A, Poston M, Cisneros R, et al. Circle of Willis atherosclerosis: association with Alzheimer's disease, neuritic plaques and neurofibrillary tangles. Acta Neuropathol Jan 2007;113(1):13-21.
[58] Kalaria RN. The role of cerebral ischemia in Alzheimer's disease. Neurobiol Aging Mar–Apr 2000;21(2):321-30.
[59] Petrovitch H, White LR, Izmirilian G, Ross GW, Havlik RJ, Markesbery W, et al. Midlife blood pressure and neuritic plaques, neurofibrillary tangles, and brain weight at death: the HAAS. Honolulu-Asia aging Study. Neurobiol Aging Jan–Feb 2000;21(1):57-62.
[60] Kawai M, Kalaria RN, Harik SI, Perry G. The relationship of amyloid plaques to cerebral capillaries in Alzheimer's disease. Am J Pathol Dec 1990;137(6):1435-46.
[61] Cai Y, Xiong K, Zhang XM, Cai H, Luo XG, Feng JC, et al. Beta-secretase-1 elevation in aged monkey and Alzheimer's disease human cerebral cortex occurs around the vasculature in partnership with multisystem axon terminal pathogenesis and beta-amyloid accumulation. Eur J Neurosci Oct 2010;32(7):1223-38.
[62] Attems J, Yamaguchi H, Saido TC, Thal DR. Capillary CAA and perivascular Abeta-deposition: two distinct features of Alzheimer's disease pathology. J Neurol Sci Dec 15 2010;299(1–2):155-62.
[63] Roman GC, Kalaria RN. Vascular determinants of cholinergic deficits in Alzheimer disease and vascular dementia. Neurobiol Aging Dec 2006;27(12):1769-85.
[64] Keverne JS, Low WC, Ziabreva I, Court JA, Oakley AE, Kalaria RN. Cholinergic neuronal deficits in CADASIL. Stroke Jan 2007;38(1):188-91.
[65] Faraci FM. Reactive oxygen species: influence on cerebral vascular tone. J Appl Physiol Feb 2006;100(2):739-43.
[66] Miller AA, Drummond GR, Schmidt HH, Sobey CG. NADPH oxidase activity and function are profoundly greater in cerebral versus systemic arteries. Circ Res Nov 11 2005;97(10):1055-62.
[67] Bennett S, Grant MM, Aldred S. Oxidative stress in vascular dementia and Alzheimer's disease: a common pathology. J Alzheimers Dis 2009;17(2):245-57.
[68] Massaad CA, Amin SK, Hu L, Mei Y, Klann E, Pautler RG. Mitochondrial superoxide contributes to blood flow and axonal transport deficits in the Tg2576 mouse model of Alzheimer's disease. PLoS One 2010;5(5):e10561.
[69] Weller RO, Subash M, Preston SD, Mazanti I, Carare RO. Perivascular drainage of amyloid-beta peptides from the brain and its failure in cerebral amyloid angiopathy and Alzheimer's disease. Brain Pathol Apr 2008;18(2):253-66.
[70] Weller RO, Djuanda E, Yow HY, Carare RO. Lymphatic drainage of the brain and the pathophysiology of neurological disease. Acta Neuropathol Jan 2009;117(1):1–14.
[71] Deane R, Bell RD, Sagare A, Zlokovic BV. Clearance of amyloid-beta peptide across the blood–brain barrier: implication for therapies in Alzheimer's disease. CNS Neurol Disord Drug Targets Mar 2009;8(1):16-30.
[72] Shibata M, Yamada S, Kumar SR, Calero M, Bading J, Frangione B, et al. Clearance of Alzheimer's amyloid-ss(1–40) peptide from brain by LDL receptor-related protein-1 at the blood–brain barrier. J Clin Invest Dec 2000;106(12):1489-99.
[73] Sagare A, Deane R, Bell RD, Johnson B, Hamm K, Pendu R, et al. Clearance of amyloid-beta by circulating lipoprotein receptors. Nat Med Sep 2007;13(9):1029-31.
[74] Firbank MJ, Burton EJ, Barber R, Stephens S, Kenny RA, Ballard C, et al. Medial temporal atrophy rather than white matter hyperintensities predict cognitive decline in stroke survivors. Neurobiol Aging Nov 2007;28(11):1664-9.
[75] Firbank MJ, He J, Blamire AM, Singh B, Danson P, Kalaria RN, et al. Cerebral blood flow by arterial spin labeling in poststroke dementia. Neurology Apr 26 2011;76(17):1478-84.
[76] Gemmell E, Bosomworth H, Allan L, Hall R, Khundakar A, Oakley AE, et al. Hippocampal neuronal atrophy and cognitive function in delayed poststroke and aging-related dementias. Stroke March 2012;43:808-14.
[77] Nishio K, Ihara M, Yamasaki N, Kalaria RN, Maki T, Fujita Y, et al. A mouse model characterizing features of vascular dementia with hippocampal atrophy. Stroke Jun 2010;41(6):1278-84.
[78] Kalaria RN, Bhatti SU, Palatinsky EA, Pennington DH, Shelton ER, Chan HW, et al. Accumulation of the beta amyloid precursor protein at sites of ischemic injury in rat brain. Neuroreport Feb 1993;4(2):211-4.
[79] Kitaguchi H, Tomimoto H, Ihara M, Shibata M, Uemura K, Kalaria RN, et al. Chronic cerebral hypoperfusion accelerates amyloid beta deposition in APPSwInd transgenic mice. Brain Res Oct 19 2009;1294:202-10.
[80] Yamada M, Ihara M, Okamoto Y, Maki T, Washida K, Kitamura A, et al. The influence of chronic cerebral hypoperfusion on cognitive function and amyloid beta metabolism in APP overexpressing mice. PLoS One 2011;6(1):e16567.
[81] Okamoto Y, Yamamoto T, Kalaria RN, Senzaki H, Maki T, Hase Y, et al. Cerebral hypoperfusion accelerates cerebral amyloid angiopathy and promotes cortical microinfarcts. Acta Neuropathol Dec 2012;123:381-94.
[82] Solfrizzi V, Frisardi V, Seripa D, Logroscino G, Imbimbo BP, D'Onofrio G, et al. Mediterranean diet in predementia and dementia syndromes. Curr Alzheimer Res Aug 2011;8(5):520-42.
[83] Morris MC, Evans DA, Bienias JL, Tangney CC, Bennett DA, Wilson RS, et al. Consumption of fish and n−3 fatty acids and risk of incident Alzheimer disease. Arch Neurol Jul 2003;60(7):940-6.
[84] van Gelder BM, Tijhuis M, Kalmijn S, Kromhout D. Fish consumption, n−3 fatty acids, and subsequent 5-y cognitive decline in elderly men: the Zutphen Elderly Study. Am J Clin Nutr Apr 2007;85(4):1142-7.
[85] Kidd PM. Alzheimer's disease, amnestic mild cognitive impairment, and age-associated memory impairment: current understanding and progress toward integrative prevention. Altern Med Rev Jun 2008;13(2):85–115.
[86] Scarmeas N, Luchsinger JA, Schupf N, Brickman AM, Cosentino S, Tang MX, et al. Physical activity, diet, and risk of Alzheimer disease. JAMA Aug 12 2009;302(6):627-37.
[87] Lazarov O, Robinson J, Tang YP, Hairston IS, Korade-Mirnics Z, Lee VM, et al. Environmental enrichment reduces Abeta levels and amyloid deposition in transgenic mice. Cell Mar 11 2005;120(5):701-13.

[88] Maesako M, Uemura K, Kubota M, Kuzuya A, Sasaki K, Asada M, et al. Environmental enrichment ameliorated high-fat diet-induced Abeta deposition and memory deficit in APP transgenic mice. Neurobiol Aging Dec 2011;33:1011:e1011-23.
[89] Baker LD, Bayer-Carter JL, Skinner J, Montine TJ, Cholerton BA, Callaghan M, et al. High-intensity physical activity modulates diet effects on cerebrospinal amyloid-beta levels in normal aging and mild cognitive impairment. J Alzheimers Dis Oct 2012;28: 137-46.
[90] Hofman A, Ott A, Breteler MM, Bots ML, Slooter AJ, van Harskamp F, et al. Atherosclerosis, apolipoprotein E, and prevalence of dementia and Alzheimer's disease in the Rotterdam Study. Lancet Jan 18 1997;349(9046):151-4.
[91] Luchsinger JA, Reitz C, Honig LS, Tang MX, Shea S, Mayeux R. Aggregation of vascular risk factors and risk of incident Alzheimer disease. Neurology Aug 23 2005;65(4):545-51.
[92] Velliquette RA, O'Connor T, Vassar R. Energy inhibition elevates beta-secretase levels and activity and is potentially amyloidogenic in APP transgenic mice: possible early events in Alzheimer's disease pathogenesis. J Neurosci Nov 23 2005;25(47):10,874-83.

Acta Neuropathol (2012) 123:381–394
DOI 10.1007/s00401-011-0925-9

ORIGINAL PAPER

Cerebral hypoperfusion accelerates cerebral amyloid angiopathy and promotes cortical microinfarcts

Yoko Okamoto · Toru Yamamoto · Raj N. Kalaria · Hideto Senzaki · Takakuni Maki · Yoshiki Hase · Akihiro Kitamura · Kazuo Washida · Mahito Yamada · Hidefumi Ito · Hidekazu Tomimoto · Ryosuke Takahashi · Masafumi Ihara

Received: 11 July 2011 / Revised: 29 November 2011 / Accepted: 1 December 2011 / Published online: 15 December 2011

Abstract Cortical microinfarcts (CMIs) observed in brains of patients with Alzheimer's disease tend to be located close to vessels afflicted with cerebral amyloid angiopathy (CAA). CMIs in Alzheimer's disease are preferentially distributed in the arterial borderzone, an area most vulnerable to hypoperfusion. However, the causal association between CAA and CMIs remains to be elucidated. This study consists of two parts: (1) an observational study using postmortem human brains ($n = 31$) to determine the association between CAA and CMIs, and (2) an experimental study to determine whether hypoperfusion worsens CAA and induces CMIs in a CAA mouse model. In postmortem human brains, the density of CMIs was 0.113/cm^2 in mild, 0.584/cm^2 in moderate, and 4.370/cm^2 in severe CAA groups with a positive linear correlation ($r = 0.6736$, $p < 0.0001$). Multivariate analysis revealed that, among seven variables (age, disease, senile plaques, neurofibrillary tangles, CAA, atherosclerosis and white matter damage), only the severity of CAA was a significant multivariate predictor of CMIs ($p = 0.0022$). Consistent with the data from human brains, CAA model mice following chronic cerebral hypoperfusion due to bilateral common carotid artery stenosis induced with 0.18-mm diameter microcoils showed accelerated deposition of leptomeningeal amyloid β (Aβ) with a subset of them developing microinfarcts. In contrast, the CAA mice without hypoperfusion exhibited very few leptomeningeal Aβ depositions and no microinfarcts by 32 weeks of age. Following 12 weeks of hypoperfusion, cerebral blood flow decreased by 26% in CAA mice and by 15% in wild-type mice, suggesting impaired microvascular function due to perivascular Aβ accumulation after hypoperfusion. Our results suggest that cerebral hypoperfusion accelerates CAA, and thus promotes CMIs.

Keywords Cerebral amyloid angiopathy · Cortical microinfarcts · Tg-SwDI · Bilateral common carotid artery stenosis

Electronic supplementary material The online version of this article (doi:10.1007/s00401-011-0925-9) contains supplementary material, which is available to authorized users.

Y. Okamoto · T. Maki · Y. Hase · A. Kitamura · K. Washida · M. Yamada · H. Ito · R. Takahashi · M. Ihara (✉)
Department of Neurology, Kyoto University Graduate School of Medicine, 54 Kawaharacho, Shogoin, Sakyo, Kyoto 606-8507, Japan
e-mail: ihara@kuhp.kyoto-u.ac.jp

T. Yamamoto · H. Senzaki
Osaka Saiseikai Nakatsu Hospital, Osaka, Japan

R. N. Kalaria
Institute for Ageing and Health, WRC, Campus for Ageing and Vitality, Newcastle University, Newcastle upon Tyne, UK

H. Tomimoto
Department of Neurology, Mie University Graduate School of Medicine, Tsu, Mie, Japan

Introduction

Cortical microinfarcts (CMIs) are frequently observed in the brains of Alzheimer's disease (AD) patients [33, 41], and tend to be located in the vascular territory of leptomeningeal arteries or cortical arterioles exhibiting cerebral amyloid angiopathy (CAA), a pathological hallmark of AD [20, 33]. Furthermore, CMIs in AD are preferentially distributed in the arterial borderzone, an area particularly vulnerable to hypoperfusion [41], suggesting a causal relationship between CAA and CMIs, with hypoperfusion

serving as a mediating factor. Indeed, our neuropathological study has shown that CMIs are present predominantly in the arterial borderzone between the middle and posterior cerebral artery territories in AD patients [33], which may coincide with the relative predilection of CAA pathology in posterior brain regions [42].

Nevertheless, the previous reports on the association between CAA and CMIs in AD brains have been conflicting [12, 24, 34, 40]; some studies have reported an association [34, 40] while others have found no such link [12, 24] (Supplementary Table 1). One of the plausible explanations for the disparity in the previous reports is the difficulty in assessing how the various AD-related pathologies, such as senile plaques (SPs), neurofibrillary tangles (NFTs), and CAA contribute to CMI development. Another complication arising from the findings is that these pathological changes can also be interdependent on concomitant atherosclerosis or arteriolosclerosis [34, 46]. Such difficulties are exemplified by the fact that SPs and CAA appear in close proximity in AD patients [48], though on a case-by-case level, an inverse correlation between CAA and plaque density is apparent [50].

The purpose of this study was to elucidate the possible association between the burden of CMIs and CAA by investigating postmortem brains exhibiting CAA where the final neuropathological diagnoses included not only AD but also other neurodegenerative disorders and vascular cognitive impairment. By avoiding a biased selection of postmortem brains, we anticipated this study would enable comparison of AD and non-AD patients that are accompanied by pathologically proven CAA to investigate the association between CMIs and CAA.

To explore whether chronic cerebral hypoperfusion is associated with the relationship between CMIs and CAA, we used a transgenic mouse CAA model that expresses human vasculotropic Swedish/Dutch/Iowa mutant amyloid precursor protein (APP) (Tg-SwDI mice) [11] and subjected them to bilateral common carotid artery stenosis (BCAS) to mimic chronic cerebral hypoperfusion [37]. By combining the animal investigations with postmortem human work, we aimed to reveal the underlying mechanisms in the relationship between CMIs and CAA.

Materials and methods

Postmortem human brain material

Two hundred seventy-five autopsied brains were obtained from Kyoto University Hospital and Osaka Saiseikai Nakatsu Hospital from 1992 to 2009 through a process approved by an institutional research committee. As we described previously [1, 21], neuropathological diagnoses were made by thorough histopathological examination of extensively sampled brain sections (Supplementary Fig. 1). In brief, in all brains at least 20 different samples, including anteroinferior frontal region, anterior cingulate region, middle frontal gyrus, superior frontal gyrus, precentral gyrus, superior and middle temporal gyri, amygdala, hippocampus, entorhinal cortex, supramarginal sulcus, occipital lobe, basal ganglia, thalamus, cerebellum, and at least 3 levels of the brainstem, were systematically taken from the formalin-fixed brains (Supplementary Fig. 1). Among the 275 patients, 31 patients were pathologically proved to have CAA by hematoxylin and eosin (H&E) staining and then by β-amyloid (Aβ) immunostaining, all of which were included in this study. Autopsies were performed at 12.9 ± 11.9 h (mean ± SD) (range 1.5–45.5 h) after death. The average fixation time was 37 ± 57 days (range 6–330 days) (Supplementary Table 2).

Clinical and pathological diagnosis

The 31 patients consisted of 14 AD (mean ± SD, 81 ± 8-year old) and 17 non-AD patients (78 ± 8-year old). The breakdown of the 17 non-AD patients is listed in Supplementary Table 2. The premortem clinical diagnoses, causes of death, vascular risk factors, postmortem pathological diagnoses and other demographic and pathological data of the 31 patients are also shown in Supplementary Table 2.

The clinical diagnosis of dementia met the criteria of the Diagnostic and Statistical Manual of Mental Disorders IV [3]. The neuropathological diagnoses of AD were made if the postmortem brains revealed the presence of frequent neuritic plaques in the neocortex (Consortium to Establish a Registry for Alzheimer's Disease, CERAD) [29], and NFT stage was no less than IV, according to the Braak and Braak neuropathological staging of Alzheimer-related changes [7, 8] as assessed with modified Bielschowsky staining. Two observers (T.Y. and Y.O.) assessed SP and NFT stage individually, and if required, a joint assessment was scrutinized under a two headed microscope. The diagnosis of diffuse Lewy body disease was also made by thorough histopathological examination of extensively sampled brain sections [27]. The diagnosis of subcortical ischemic vascular dementia was made clinically [5], and was retrospectively found to meet the pathological criteria outlined by Kalaria et al. [19]: (1) the presence of bilateral diffuse white matter lesions, (2) the presence of lacunar infarctions in the perforator territory, and (3) the presence of arteriolosclerosis.

Grading of atherosclerosis

At autopsy, the atherosclerosis stage was consistently graded by one of the authors (T.Y.). The degree of atherosclerosis at

skull base was classified into four grades: 'normal' (no atherosclerosis), 'mild' (the presence of patchy atheroma), 'moderate' (a severity that is intermediate between mild and severe), or 'severe' (the presence of atheroma along the entire length of the vessels). The above staging was re-examined and confirmed by another author (Y.O.) using the autopsy report and macroscopic images taken at autopsy.

Tinctorial and immunohistochemical staining

Tissue blocks were obtained from the frontal, temporal, parietal, and occipital lobes (Supplementary Fig. 1). The blocks were embedded in paraffin and sectioned at 12 μm thickness for Congo Red staining, and 6 μm thickness for other staining on a microtome. To minimize variability in staining intensity, tissue sections were prepared by the same technician and stained with or using freshly prepared tinctorial and buffer solutions. Routine histological assessment was carried out with Congo Red, H&E, Klüver-Barrera (KB), modified Bielschowsky, and Gallyas staining. Pearls-Stieda staining was added as it was needed. The rest of the blocks were used for immunohistochemistry, involving sequential incubation with primary antibody, appropriate biotinylated secondary antibody (diluted 1:200, Vector Laboratories, Burlingame, CA, USA), and avidin–biotin–peroxidase complex (1:200, Vector Laboratories) in 0.1 M phosphate-buffered saline (PBS, pH 7.4). The sections were visualized with 0.01% diaminobenzidine tetrahydrochloride and 0.005% H_2O_2 in 50 mM Tris–HCl (pH 7.6). The primary antibodies were mouse anti-$A\beta_{8-17}$ (6F/3D) (1:100, Novocastra, Newcastle, UK), rabbit anti-cow glial fibrillary acidic protein (GFAP) (1:200, DAKO, Glostrup, Denmark), mouse anti-human paired helical filament-tau (AT8; 1:200, Thermo Scientific, Rockford, IL, USA), and mouse anti-cluster of differentiation 68 (CD68) (1:100, DAKO) antibodies.

Senile plaque and neurofibrillary tangle burden

The burden of neuritic plaques was classified into 'none', 'sparse', 'moderate', and 'frequent' categories in the cortical sections stained with the modified Bielschowsky staining according to CERAD protocol [29]. The stage of NFTs was assessed according to the Braak and Braak neuropathological staging of Alzheimer-related changes [7, 8]. In this study, we used 6 μm thick paraffin sections using the modified Bielschowsky method as we have previously reported [52]; because, the modified Bielschowsky method is far more effective over other silver staining methods in detecting NFTs.

Staging of CAA

For staging of CAA, 12 μm thick sections were stained with Congo Red and viewed with polarized light [13, 42]. CAA was classified into CAA Type 1 (affected capillaries with or without larger cerebral vessel involvement) and CAA Type 2 (affected leptomeningeal arteries, cortical arteries/arterioles, or rarely veins), as proposed by Attems et al. [4]. CAA Type 2 was further analyzed, and was divided into three grades proposed by Vonsattel et al. [44]: those with 'mild' (focal Aβ deposits in the smooth muscle layer of the vessel walls), 'moderate' (circumferential Aβ deposits in the smooth muscle layer of the vessel walls), and 'severe' (extensive Aβ deposition with morphological changes such as microaneurysms, fibrinoid necrosis, double barreling, inflammation, thrombus, or hemorrhage) (Fig. 1). When several grades were observed in one case, the dominant grade represented the case.

Definition and quantitative analysis of CMI

CMIs were analyzed in the same sections that were used for pathological confirmation of CAA. CMIs were defined as cerebral cortex lesions visible only microscopically [19] and usually accompanied by reactive glial proliferation. Regions of interest with evidence of expanded Virchow-Robin space or microabscess as well as those accompanied by hemorrhagic changes or cortical laminar necrosis on H&E staining were excluded from analysis. Following further confirmation of CMIs with immunohistochemistry for GFAP and CD68, we determined the density of CMIs using a method reported previously [33]. In brief, the number of CMIs in each lobe was counted in sections stained with H&E. Images of the H&E stained slides were scanned (GT-X770 EPSON, Nagano, Japan). The cerebral cortices were outlined on each slide and the areas were measured using the ImageJ software package (image processing and analysis in JAVA, ImageJ bundled with JAVA 1.43, NIH, USA). The number of CMIs per cm^2 of the cortex was calculated as a measure of CMI density. The CMI density in the frontal cortex was the mean of the values obtained from the five areas (anteroinferior frontal region, anterior cingulate region, middle frontal gyrus, superior frontal gyrus, precentral gyrus), and that in the temporal cortex was the mean of the values obtained from the two areas (lateral and medial temporal). The CMI density in the parietal cortex was obtained from the parietal supramarginal gyrus, and that in the occipital cortex was obtained from the occipital calcarine cortex (Supplementary Fig. 1).

Assessment of white matter changes

Using H&E- and KB-stained slides cut coronally at the level of mid-hippocampus, parietal, and occipital lobes, we classified white matter lesions into four grades as reported previously [9, 17]: those with 'normal' (normal white

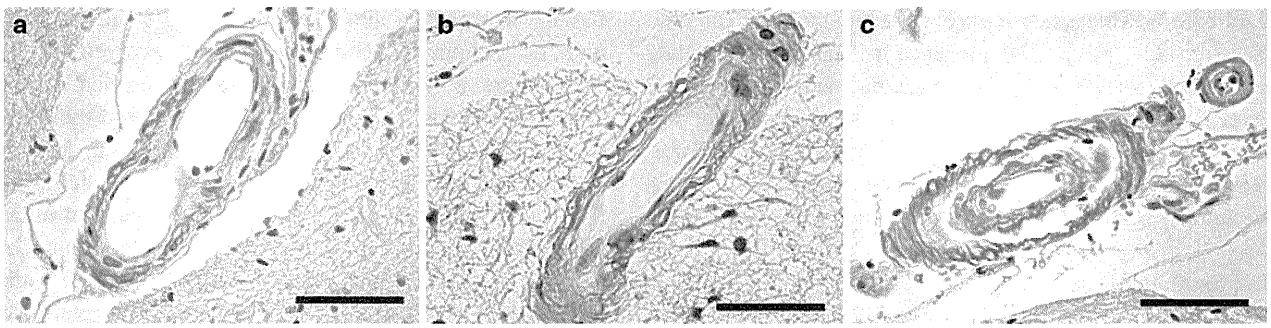

Fig. 1 Representative photomicrographs of various grades of CAA. Congo Red staining showing mild CAA (**a**), moderate CAA (**b**), and severe CAA associated with double barreling (**c**). *Bars* indicate 100 μm in **a** and **c**, and 50 μm in **b**

matter), 'mild' (no appreciable reduction in axonal meshwork density, and a slightly increased number of reactive astrocytes), 'moderate' (a slight reduction of axonal meshwork density, a reduction of oligodendroglial cell nuclei, and a further increased number of reactive astrocytes), and 'severe' (a marked reduction of myelin, axons and oligodendroglial cell nuclei with relatively marked astrocytic reaction, loosely scattered macrophages but no complete cerebral infarction).

Experimental animals

We used transgenic mice, C57BL/6-Tg(Thy1-APPSwDutIowa)BWevn/J [11] (Jackson Laboratory, Bar Harbor, ME, USA), which overexpress the neuronally derived human APP gene, encoding the Swedish p.K670N/M671L, Dutch p.E693Q and Iowa p.D694N mutations, under the control of the mouse thymus cell antigen 1 (Thy1) promoter. Generally, Thy1-driven exogenous gene expression is not altered by hypoxic/ischemic condition [26, 43]. The mice were screened for transgene expression by polymerase chain reaction, and heterozygous mice were mated with non-transgenic C57BL/6J mice (Japan SLC, Hamamatsu, Japan). All mice were given free access to food and water.

Surgical procedures and rearing methods

Male heterozygous mice were subjected to either sham or BCAS operation using microcoils [22, 30, 32, 37, 38]. Body weight and rectal temperature were measured, and blood pressure was monitored from the tail artery of the sham- or BCAS-operated mice. Under anesthesia with 1.5% isoflurane, the common carotid arteries were exposed through a midline cervical incision, and a microcoil with an internal diameter of 0.18 mm was applied to the bilateral common carotid arteries. Sham-operated animals underwent bilateral exposure of the common carotid arteries without inserting the microcoil. Rectal temperature was maintained between 36.5 and 37.5°C, and body weight monitored until the animals were euthanized. After the operation, the mice were housed in cages with a 12-h light/dark cycle (lights on at 7:00 a.m.). Three animal groups were prepared in this experiment (6 groups, $n = 4$–7 per group, $n = 31$ in total; detailed information given in Supplementary Table 3). The timing of sham/BCAS and the duration of cerebral hypoperfusion are described in Supplementary Fig. 2. In brief, Tg-SwDI mice were subjected to sham or BCAS operation at 10, 16, and 20 weeks of age, and they were subsequently killed at 18, 24, and 32 weeks of age, respectively, to assess histology. Wild-type age-matched C57BL/6J mice ($n = 5$ per group) were also subjected to BCAS operation. The number of mice used in this study was minimized for ethical reasons, and all procedures were performed in accordance with the guidelines for animal experimentation from the ethical committee of Kyoto University.

Systolic blood pressure and cerebral blood flow measurements

Mice were thermostatically controlled at 37°C on a warming pad and cerebral blood flow (CBF) and systolic blood pressure (SBP) recorded preoperatively and postoperatively at 32 weeks of age (12 weeks after BCAS or sham operation). Mean value of ten replicate measurements of CBF or SBP was determined for each mouse. The SBP was monitored in conscious mice by the tail-cuff method (MK-2000ST; Muromachi Co., Kyoto, Japan). The CBF was measured in identically sized regions of interest (900 pixels) located 1 mm posterior and 2 mm lateral from the bregma by Laser speckle blood flow imager (Omega Zone; Omegawave, Tokyo, Japan) under anesthesia with 1.5% isoflurane after the periosteum was widely removed with fine-tip forceps and calibration was carried out with a calibration reference device (Calibrator S/N 080715-5, Omegawave, Inc., Tokyo, Japan). CBF values were expressed as a percentage of the preoperative value. Since

repetitive CBF measurement leads to fibrous scar tissue build up and bone opacification, CBF was measured only at two time points.

Histological investigation in mice

Mice were anesthetized with sodium pentobarbital (50 mg/kg, intraperitoneal) and transcardially perfused with 0.01 M phosphate buffer (PB) in normal saline. The removed brains were immersion-fixed in 4% paraformaldehyde in 0.1 M PB, and embedded in paraffin. The brains were then sliced into 6 μm thick sagittal sections at 1, 2, 3, and 4 mm lateral from the midline, and subjected to H&E and modified Bielschowsky staining. Immunohistochemical staining was performed according to the same protocol as human tissue. Mouse anti-$A\beta_{1-40}$ (BA27) (Wako amyloid kit, Wako, Osaka, Japan), mouse anti-$A\beta_{1-42}$ (BC05) (Wako amyloid kit, Wako), and mouse anti-$A\beta_{5-10}$ (6E10) (1:500, Covance, Princeton, NJ, USA) antibodies were used.

Densitometric analysis of mouse brains

The Aβ-stained slides were captured with a digital camera (BZ-9000 KEYENCE, Osaka, Japan). Then, using the ImageJ software, the densitometric analysis of Aβ was performed blindly to animal groups by setting regions of interest in the cerebral cortex, the hippocampus, and the leptomeninges with the identical threshold in the Aβ (6E10)-immunostained sections. Leptomeningeal vascular, as well as pial, Aβ accumulations were jointly analyzed as 'leptomeningeal Aβ'.

Statistical analysis

For human samples, numerical scores were computed from the data analysis as follows: age, 65- to 93-year old; disease group, AD = 1 or non-AD = 0; the grade of atherosclerosis, 0–3; the severity of CAA, 1–3; SP burden, 0–3; NFT stage, 0–6; and the grade of WML, 0–3. We first performed univariate analysis to determine whether age, disease type, or the above pathological changes were predictive of CMI formation using Fisher's exact test. Next, multivariate analysis was performed while taking into account the effects of all variables on the parameters measured, including CMI formation.

In mice, Student's t test was used to evaluate possible differences between the sham- and BCAS-operated mice groups at each time point, and two-way ANOVA was used to test for the effect of age and operation on Aβ deposition in the hippocampus, cerebral cortex, and leptomeninges. Differences with $p < 0.05$ were considered statistically significant in all analyses used.

Results

The grade of CAA and atherosclerosis, SP and NFT stage, the degree of WML, and the CMI densities in the autopsy series are shown in Table 1.

Capillary CAA

Capillary CAA was found in only one patient (Table 1, Patient no. 26). In this patient, findings of Aβ depositions in the leptomeningeal arteries and cortical arterioles were also prominent. In the remaining 30 patients, capillary CAA was undetectable with H&E staining and Aβ immunohistochemistry. In the following analyses, therefore, only CAA Type 2 was graded.

Cortical microinfarcts

CMIs were present along the sulcus in the superficial cortex with variable frequency among the postmortem brains (Fig. 2a, b). The average microinfarct diameter was approximately 200 μm (range 100–500 μm). Some lesions were recently formed, with the presence of GFAP-positive gemistocytic astroglial cells and CD68-positive microglia/macrophages (Fig. 2c–e), while others were relatively old with induction of fibrillary astrocyte gliosis. Thrombus formation was found in one patient with severe CAA (Table 1, Patient no. 13).

Most CMIs (>90%) were located in close proximity (~1 cm) to Aβ-deposited vessels (Fig. 3a–c). Around ischemic foci, such as CMIs or necrosis, SPs were sometimes not present (Fig. 3c). Furthermore, in and around ischemic foci, vascular Aβ deposition appeared to increase in intensity (Fig. 3a–c).

CMI density in AD and non-AD patients

The results of the univariate analyses are shown in Table 2. The mean CMI density within the four cortical lobes was not significantly different ($r = -0.1007$, $p = 0.5900$) in AD group (0.71/cm^2) and non-AD group (1.12/cm^2) (Fig. 4a). When AD and non-AD groups were combined, CMI density in the frontal, temporal, parietal, and occipital lobes was 1.02, 0.65, 1.18, and 0.93/cm^2, respectively (Fig. 4b). There were no significant differences in the CMI density within the four cortical lobes. CMI density in the frontal, temporal, parietal, and occipital lobes was 1.32, 0.29, 1.03, and 0.30/cm^2, respectively, in the AD group, while in the non-AD group the CMI density was 0.76, 0.97, 1.29, and 1.44/cm^2, respectively (Fig. 4c).

CMI density was 0.11/cm^2 in mild, 0.58/cm^2 in moderate, and 4.37/cm^2 in severe CAA groups, meaning it became greater as CAA severity increased ($r = 0.6736$,